

Carbon Accumulation and Storage in a Temperate Coastal Lagoon under the Influence of Recent Climate Change (Northwestern Adriatic Sea)

Roberta Guerra¹, Andrea Pasteris¹, and Simona Simoncelli²

¹University of Bologna

²INGV

November 21, 2022

Abstract

Pialassa Baiona is a shallow temperate coastal lagoon influenced by a variety of factors, including regional climate change and local anthropogenic disturbances. To better understand how these factors influenced modern organic carbon (OC) sources and accumulation, we measured OC as well as stable carbon isotopes ($d^{13}C$) in ^{210}Pb -dated sediments within a vegetated saltmarsh habitat and a human impacted habitat. Relative Sea Level (RSL) at the nearby tide gauge station data and four different Sea Surface Temperature (SST) data sets were analyzed starting from 1900 to assess the potential effect of sea ingression and warming on the coastal lagoon sedimentary process. The source contribution calculated from the MixSIAR Bayesian model revealed a mixed sedimentary organic matter (OM) composition dominated by increasing marine-derived OM after the 1950s, parallel with decreasing autochthonous saltmarsh vegetation (*Juncus* spp.) in the saltmarsh habitat and riverine-estuarine-derived OM in the impacted habitat. RSL rise in the area (8.7 ± 0.5 mm yr^{-1} in the period 1900-2014) has been mainly driven by the land subsidence, especially during the central decades of the last century, enhancing the sea ingression in the lagoon. Annual SST anomalies present, starting from the eighties, a continuous warming tendency from 0.034 ± 0.01 to 0.044 ± 0.009 degC yr^{-1} . No direct effect on sedimentary properties was detected; however, RSL influenced OM sediment properties, although this effect was different between the two habitats.

Hosted file

guerraetal_carbon storage and burial_suppinfo_8sep2021.docx available at <https://authorea.com/users/526814/articles/596481-carbon-accumulation-and-storage-in-a-temperate-coastal-lagoon-under-the-influence-of-recent-climate-change-northwestern-adriatic-sea>

1
2 **Carbon Accumulation and Storage in a Temperate Coastal Lagoon under the Influence of Recent**
3 **Climate Change (Northwestern Adriatic Sea)**
4

5 **Roberta Guerra^{1,2}, Simona Simoncelli³, and Andrea Pasteris^{2,4}**

6 ¹Department of Physics and Astronomy, University of Bologna, Bologna, Italy, ²Interdepartmental Research
7 Centre for Environmental Sciences (CIRSA), University of Bologna, Ravenna Campus, 48123 Ravenna, Italy,
8 ³National Institute of Geophysics and Volcanology (INGV), Bologna, Italy, ⁴Department of Biological,
9 Geological, and Environmental Sciences (BiGeA), University of Bologna, Bologna, Italy.

10
11 Corresponding author: Roberta Guerra (roberta.guerra@unibo.it)
12

13 **Key Points:**

- 14 • The relative contribution of allochthonous marine-derived organic matter increased over the years
15 reflecting local relative sea level
- 16 • Decreased contribution of autochthonous-derived organic matter from C3 vegetation is evident in the
17 saltmarsh habitat since the 1950s
- 18 • Relative sea level rise influenced sedimentary organic matter although this effect was different between
19 and within habitats
20

Abstract

Pialassa Baiona is a shallow temperate coastal lagoon influenced by a variety of factors, including regional climate change and local anthropogenic disturbances. To better understand how these factors influenced modern organic carbon (OC) sources and accumulation, we measured OC as well as stable carbon isotopes ($\delta^{13}\text{C}$) in ^{210}Pb -dated sediments within a vegetated saltmarsh habitat and a human impacted habitat. Relative Sea Level (RSL) at the nearby tide gauge station data and four different Sea Surface Temperature (SST) data sets were analyzed starting from 1900 to assess the potential effect of sea ingression and warming on the coastal lagoon sedimentary process. The source contribution calculated from the MixSIAR Bayesian model revealed a mixed sedimentary organic matter (OM) composition dominated by increasing marine-derived OM after the 1950s, parallel with decreasing autochthonous saltmarsh vegetation (*Juncus* spp.) in the saltmarsh habitat and riverine-estuarine-derived OM in the impacted habitat. RSL rise in the area ($8.7\pm 0.5 \text{ mm yr}^{-1}$ in the period 1900-2014) has been mainly driven by the land subsidence, especially during the central decades of the last century, enhancing the sea ingression in the lagoon. Annual SST anomalies present, starting from the eighties, a continuous warming tendency from 0.034 ± 0.01 to $0.044\pm 0.009^\circ\text{C yr}^{-1}$. No direct effect on sedimentary properties was detected; however, RSL influenced OM sediment properties, although this effect was different between the two habitats.

Plain Language Summary

Coastal vegetated ecosystems (mangroves, saltmarshes, seagrasses) are highly efficient in removing carbon dioxide from the atmosphere through plant growth and thus play an important role in climate regulation, limiting the greenhouse effect. The term “blue carbon” has been devised to refer to carbon captured from the atmosphere and stored as organic matter in the sediments of these habitats. On the other hand, climate changes and human activities can affect coastal ecosystems and the quality and quantity of blue carbon. The goal of the present study was to analyze how the characteristic of the organic matter stored in the sediment of a Mediterranean coastal lagoon changed over the time from year 1850 to year 2010. These changes were compared with changes in sea water temperature and Relative Sea Level over the same period. Results showed that the importance of marine organic matter entering the lagoon from outside increased after the 1950s, while the contribution of organic matter produced inside the lagoon decreased. It is likely that Relative Sea Level, dominated by subsidence in the area, enhanced sea ingression and thus inputs of marine organic carbon. Such changes will continue to have an impact on the accumulation and storage of blue carbon.

1 Introduction

Carbon captured and stored in sediments from coastal vegetated habitats (wetlands, saltmarshes, tidal flats), where the rates of organic carbon (OC) accumulation from multiple sources is high, constitutes a relevant and active fraction in the global carbon sink, and plays an important role in climate regulation and mitigation (Kirwan and Mudd, 2012). However, a global inventory of this coastal ‘blue carbon’ storage remains a challenge, as observations of OC accumulation and stock in coastal ecosystems are labor intensive, expensive, scarce, and unevenly distributed, with few records even for relatively well-studied temperate areas in the Northern Hemisphere (Beaumont et al., 2014). Recent reviews (Duarte et al., 2005; Wilkinson et al., 2018) report a mean organic carbon accumulation rate of $151 \text{ g C m}^{-2} \text{ yr}^{-1}$ for saltmarshes (maximum $1720 \text{ g C m}^{-2} \text{ yr}^{-1}$), $41.4 \text{ g C m}^{-2} \text{ yr}^{-1}$ for lagoons (maximum $340 \text{ g C m}^{-2} \text{ yr}^{-1}$), and $62.9 \text{ g C m}^{-2} \text{ yr}^{-1}$ for coastal wetlands (maximum $335.8 \text{ g C m}^{-2} \text{ yr}^{-1}$) exceeding the mean burial rate of estuaries and continental shelves ($17\text{--}45 \text{ g C m}^{-2} \text{ yr}^{-1}$).

The rate of accumulation of ‘blue carbon’, mostly stored in soil and sediments within coastal vegetated ecosystems, is sensitive to rapidly changing climate factors (e.g. warming, sea level rise, inundation frequency) and non climatic anthropogenic drivers (e.g. eutrophication, landscape development) (Arriola, 2017; Cuellar-martinez et al., 2019; Ewers Lewis et al., 2018; Kelleway et al., 2017; Kirwan and Mudd, 2012; Macreadie and

Saintilan, 2019; Macreadie et al., 2013; Negandhi et al., 2019; Pendleton et al., 2012; Rogers et al., 2019; Ruiz-fernández et al., 2018; Simpson et al., 2017). Between 20 and 90% of the existing area occupied by coastal vegetated ecosystems is projected to be lost at global level by 2100, depending on sea level rise projections and warming under future emission scenarios (IPCC, 2019).

Carbon stable isotopic composition ($\delta^{13}\text{C}$) in combination with supporting geochemistry, specifically the ratio of organic carbon to total nitrogen (C/N) and total organic carbon content (OC), have been used as tracers to differentiate sources of organic matter (OM) that characteristically accumulate in sediments of coastal vegetated habitats near the Westerschelde Estuary (SW Netherlands), in Massachusetts and South Carolina (USA) (Chen et al., 2016; Goñi et al., 2003; Middelburg et al., 1997), and in Australian coastal wetlands (Saintilan et al., 2013), as well as past sea level indicators in the Thames Estuary (Khan et al., 2015b), in tidal-dominated wetlands in North West Europe (Wilson, 2017), in a back-barrier lagoon system in New Jersey, USA (Kemp et al., 2012), and in Hudson Bay, Canada (Godin et al., 2017).

The signature of bulk organic sediment $\delta^{13}\text{C}$ and C/N analysis in sediment records in European coastal vegetated habitats is primarily to distinguish between OM derived from autochthonous C3 and C4 saltmarsh vascular vegetation (i.e. coastal blue carbon; $\delta^{13}\text{C}$ -12‰ to -30‰ , C/N 5.80 to 41.10; Khan et al., 2015b), and allochthonous sources including fluvial and marine particulate organic matter (OM), the latter mainly derived from freshwater or marine phytoplankton ($\delta^{13}\text{C}$ -12‰ to -30‰ , C/N 5 to 9; Lamb et al., 2006).

There is, however, little knowledge about the spatial and historical distribution, and the sources of sedimentary OM in coastal vegetated habitats in the Mediterranean Region. In this study, carbon stable isotopic composition ($\delta^{13}\text{C}$) and C/N ratios were measured, and Pb-210 chronology reconstructed in sediment cores from two contrasting habitats (a semi-natural saltmarsh habitat and an impacted habitat) within a coastal lagoon (Pialassa Baiona) connected to the Northwestern Adriatic Sea. This temperate shallow coastal ecosystem is subject to ongoing sea level rise, sea warming (Carbognin and Tosi, 2002; Cerenzia et al., 2016; Tsimplis et al., 2012; Mariano et al., 2021), land subsidence, hydrological alterations, coastal erosion, maintenance dredging, embankments (Airoidi et al., 2016; Guerra et al., 2009).

The objectives of this work were to investigate the changes in OM accumulation and sources, and to assess the climatic factors and local anthropogenic disturbances influencing the spatial and temporal changes in OM 'blue carbon' storage in this temperate coastal lagoon (Pialassa Baiona) located in the Mediterranean Region.

2 Materials and Methods

2.1 Study area

Pialassa Baiona is a temperate coastal lagoon ($44^{\circ} 28' \text{N}$ and $44^{\circ} 31' \text{E}$) adjacent to the Northwestern Adriatic Sea (Figure 1). The area forms part of the Natura 2000 European network and is a wetland of international importance under the Ramsar Convention. The climate is hot-summer Mediterranean (Köppen-Geiger) with a continental influence, with a mean annual temperature of 14.1°C and a maximum of 29.2°C (Antolini et al., 2016). Annual rainfall ranges from 650 mm to 696 mm, mainly from October to March (Mollema and Antonellini, 2012).

The lagoon consists of shallow water bodies of saline, brackish or fresh water wetlands (~ 0.5 m average depth) completely or partially isolated by levees and crossed by a dendritic network of artificial channels dug in 1850 (~ 5 m maximum depth). The inner channels converge into a main channel connected to sea through the shipway channel. Salinity in the lagoon (25–35 psu) is mainly controlled by tidal flushing through this channel into the channels network resulting in delayed tidal oscillation and low water exchange with the open sea. On average, the water covers an area of 10 km^2 with a tidal range of 0.3–1 m, and usually vast shallow areas emerge during low tides.

The northern area is composed of unvegetated zones alternated with zones dominated by halophile species characteristic of temporarily inundated saltmarshes (*Juncus maritimus* and *Juncus acutus* and to a lesser

114 extent by *Salicornia* spp.; Merloni and Piccoli, 1999), with marginal areas with reedbeds of *Phragmites*
115 *australis* (Ferronato et al., 2016).

116 The southern area is a subtidal habitat consisting of tidal wetlands separated by discontinuous artificial
117 embankments receiving inputs from agriculture runoff, and urban and industrial wastewater discharges through
118 the main inflow channel (Airoldi et al., 2016). Vegetation is sparse and mainly present on the embankments.
119 This area has been subject to local anthropogenic disturbances (chemical and thermal pollution) resulting in
120 higher than expected concentrations of mercury, chlorinated compounds and polycyclic aromatic hydrocarbons
121 (PAHs) in sediments (Covelli et al., 2011; Guerra et al., 2014) and mussels (Capolupo et al., 2017), and
122 alteration of the benthic community (Guerra et al., 2009; Ponti et al., 2011). The high THg concentrations found
123 in the sediment of this area are in good agreement with the Hg inputs following the booming of petrochemical
124 industry located near Pialassa Baiona lagoon in the mid-1950s. Chemical plants producing acetaldehyde and
125 vinyl chloride from acetylene and using mercury salts as catalysts, released an estimated 100–200 tons of Hg
126 directly into the southern area of the lagoon during the 1958–1978 period (Miserocchi et al., 1993). In 1973,
127 wastewater treatment began, the acetaldehyde plant was shut down and the use of Hg catalysts in vinyl chloride
128 and acetaldehyde production was drastically reduced and finally discontinued by 1991 (Fabbri et al., 1998).

129

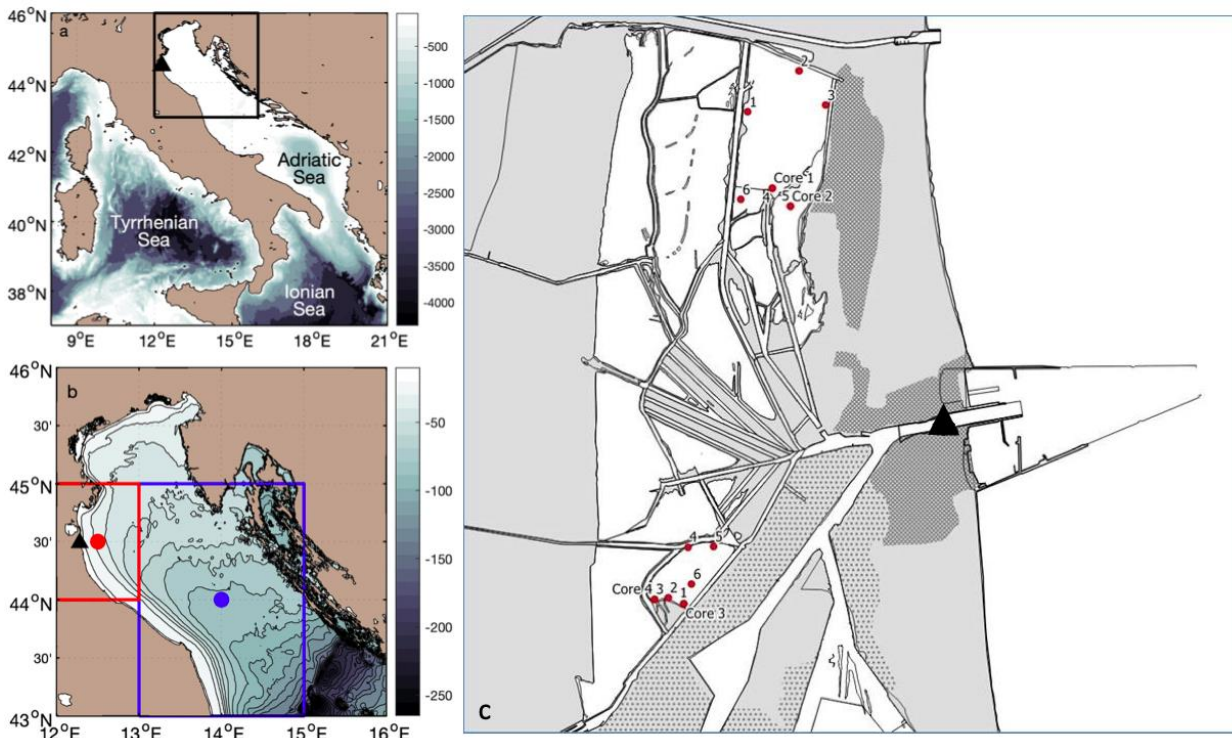


Figure 1. (a) Overview map and location of the study (black triangle) area overlain on the bathymetry from GEBCO Compilation Group (2019) GEBCO 2019 Grid. (b) Zoom in the Northern Adriatic Sea, corresponding to the black square in the left panel, and relative bathymetry. The red square and dot correspond to the HadISST and COBE-SST mesh grid, while the blue square and dot correspond to the ERSST mesh grid. (c) Map of the Pialassa Baiona coastal lagoon and station locations of surface sediment samples and core samples in the saltmarsh habitat and impacted habitat. The black triangle indicates the Porto Corsini/Marina di Ravenna tide gauge location.

2.2 Sampling

Sampling took place in April and July 2008 at two contrasting habitats within Pialassa Baiona coastal lagoon: a) a saltmarsh habitat located northward in a relatively flat area with the presence of saltmarsh vegetation, and b) a human impacted habitat located southward close to anthropogenic source inputs (Figure 1). At each habitat, sediment cores were sampled at two random locations by inserting one cylindrical Plexiglas hand corer (5 cm diameter, 50 cm long) into the sediment to a depth of 20–25 cm. The cores were extruded in the field, sectioned into 1–2 cm intervals, and analyzed for total organic carbon (OC), total nitrogen (TN), carbon isotope ratio ($\delta^{13}\text{C}$) and dry bulk density (upper 20–25 cm). In addition, a composite of two sediment cores with no evidence of physical disturbance was taken at each habitat to reconstruct the chronology of sediment accumulation. These two cores were sampled within a 1-m² area within each habitat to attenuate variation due to spatial heterogeneity (Bernal and Mitsch, 2012). Composite core intervals were bulked together to provide satisfactory amounts, which were needed for effective ²¹⁰Pb dating and dry bulk density.

Additionally, a total of 12 surface sediment samples (0–5 cm) were collected with a stainless-steel grab sampler at six stations in the saltmarsh habitat and six stations at the impacted habitat for organic matter description (OC, TN and $\delta^{13}\text{C}$) (Figure 1).

2.3 Laboratory analysis

Freeze-dried sediment samples were treated with HCl (1.5 M) to remove inorganic carbon (carbonate). Aliquots of approximately 20 mg were added into silver capsules for the measurement of total organic carbon (OC), total nitrogen (TN), and carbon isotopes ($\delta^{13}\text{C} = [({}^{13}\text{C}/{}^{12}\text{C})_{\text{sample}}/({}^{13}\text{C}/{}^{12}\text{C})_{\text{standard}} - 1] \times 1,000$) using a FINNIGAN Delta Plus XP mass spectrometer directly coupled to Thermo Fisher FLASH 2000 CHNS Elemental Analyzer. OC and TN content were expressed as the weight percentage of dried sediment, and carbon isotope results were reported in the standard delta notation (‰) with respect to the international standard Vienna Pee Dee Belemnite (VPDB). Standard deviation based on replicates of reference standard (IAEA-CH7) was $< \pm 0.2\text{‰}$.

For radiometric analysis, packed sediments (~40–50 g) were set aside for at least 21 days to allow ${}^{222}\text{Rn}$ ingrowth and to establish secular equilibrium between ${}^{226}\text{Ra}$ and its granddaughter ${}^{214}\text{Pb}$. The ${}^{210}\text{Pb}$ and ${}^{226}\text{Ra}$ activities were measured by γ -ray spectrometry, and the excess ${}^{210}\text{Pb}$ activity was estimated by subtracting the ${}^{214}\text{Pb}$ from the total ${}^{210}\text{Pb}$ activity with self-absorption corrections (Cutshall et al., 1983). Detailed information on the radiometric technique is provided in Guerra et al. (2019). The excess ${}^{210}\text{Pb}$ was used to determine ages of sediment intervals using the ‘simple’ Constant Flux Constant Sedimentation model (CF-CS; Sanchez-Cabeza and Ruiz-Fernandez, 2012). Sediment accumulation rates (SAR, cm yr^{-1}) and mass accumulation rates (MAR, $\text{g cm}^{-2} \text{yr}^{-1}$) were estimated from the profile of excess ${}^{210}\text{Pb}$ activity concentration versus sediment depth (cm) and mass sediment depth (calculated using bulk density). An aliquot of sediment was dried at 60°C to measure the water content and to calculate bulk density assuming a sediment density of 2.65 g cm^{-3} and a water density of 1.034 g cm^{-3} .

The OC accumulation rate ($\text{g OC m}^{-2} \text{yr}^{-1}$) was estimated by multiplying the OC fraction ($\% \text{OC}/100$) in each core interval by the MAR ($\text{g m}^{-2} \text{yr}^{-1}$). Total C stock (g C m^{-2}) was calculated by integrating OC accumulation rates over the c.a. last century (1900–2008).

Total mercury (THg) was determined with a Perkin Elmer Optima 3200 XL inductively coupled plasma-optical emission spectrometer coupled to a FIAS 400 hydride generation system following the US EPA method 6010C (USEPA, 2000). Sediments were digested with concentrated nitric acid (HNO_3 , Suprapur, Merck; 65%) and hydrochloric acid (HCl, Suprapur, Merck; 37%). QA/QC for THg analysis was carried out using sample replicates, method blanks, and certified reference materials (CRMs, Marine Sediment PACS-2 and MESS-3 from NIST, USA). The accuracy of the instrument was consistently within their certified range (3.04 ± 0.20 , and $0.91 \pm 0.009 \text{ } \mu\text{g g}^{-1}$, respectively), and all measured samples showed less than 10% deviation from CRMs.

2.4 Climatic data

Existing Sea Surface Temperature (SST) and Sea Level (SL) climatic data sets have been analyzed in order to assess the main climatic characteristics and changes happened after 1900 in the study region and relate them to the accumulation and variations in the pool of blue carbon through multivariate analysis.

One of the longest SL time series (1987–2014) available within the Northern Adriatic region has been recorded at the Porto Corsini/Marina di Ravenna tide gauge station (44.49°N , 12.28°E), located nearby the entrance to the Piailassa Baiona (Figure 1c), along the main shipway channel connected to the sea (Cerenzia et al., 2016; Zerbini et al., 2017). The Relative SL (RSL) data, given by the combined effect of vertical land movements and SL, used in the climatic analysis are the annual means (Figure 3) over the time period 1900–2014 analyzed and provided by Cerenzia et al., (2016). They derive from different data sources and have been properly homogenized relying upon the information on benchmarks and data overlaps. The three main RSL data sources are: (1) the Permanent Service for Mean Sea Level (PSMSL) archive for the time period 1897–1922;

(2) the Hydrology Annals of Bologna for the 1934–1979 time period and (3) the Institute for Environmental Protection and Research (ISPRA) for the period 1980–2014.

The centennial RSL change presents anomalous rate of increase ($8.5 \pm 0.2 \text{ mm yr}^{-1}$) within the Northern Adriatic and the Northern Mediterranean region. Cerenzia et al., (2016) found out that land subsidence represents the main cause of local RSL rise measured by the tide gauge due to a total land lowering from 1.8 to 0.2 m above sea level in the time period 1897–2014.

The rate of absolute SL change during the last decades, obtained by subtracting the rate of land subsidence from the rate of RSL change, is equal to $2.2 \pm 1.3 \text{ mm yr}^{-1}$, consistently with other tide gauge observations nearby (i.e. Venice, Trieste) and the estimate of 3 mm yr^{-1} computed from altimetry in the region from Bonaduce et al., (2016). Another long-term sea level trend estimate from Bruni et al., (2019) at Porto Corsini/Marina di Ravenna tide gauge gives a value of $1.25 \pm 0.16 \text{ mm yr}^{-1}$ over the time period 1873–2016.

Sea Surface Temperature gridded data sets covering the time period 1900–2018 have been retrieved from three global climatic data products with the aim to obtain a robust estimate of the long term temperature variation of the sea water entering and exiting the coastal lagoon under investigation to be used for the multivariate analysis. Three global monthly SST data sets have been considered: (1) the HadISST from Met Office Hadley Centre for Climate Prediction and Research; (2) the ERSST from NOAA National Centers for Environmental Information and (3) the COBE-SST from the Japan Meteorological Agency (JMA). These products might not fully capture regional details, as highlighted by (Li et al., 2019) thus a fourth, most recent and accurate regional satellite-based data set (Pisano et al., 2016) distributed by the Copernicus Marine Environment Monitoring Service (CMEMS) has been considered as the reference to validate the three global products and select the most representative of the area for the successive analysis. The CMEMS SST is the longest satellite SST time series (1982–2018) at 4 km resolution for the Mediterranean Basin and it is spatially complete, accurate, homogeneous and stable, i.e. free of spurious trends, all essential characteristics for products usability for climate applications. The main characteristics of the considered SST data sets have been summarized in Table 1 and detailed in the supporting information.

Table 1. Main characteristics of the SST data sets used and displayed in Figure 3.

SST Product	Reference	Time Coverage	Time resolution	Space resolution [degrees]
HadISST	(Rayner et al., 2003)	1882 onwards	monthly	1x1
ERSST	(Huang et al., 2017)	1854 onwards	monthly	2x2
COBE-SST	(Ishii et al., 2005)	1891 onwards	monthly	1x1
CMEMS REP L4	(Pisano et al., 2016)	1981–2018	daily mean	0.0417x0.0417

The closest sea grid point to the study area (Figure 1) has been selected from each global data set to first inspect the time series. HadISST and COBE-SST sea grid points are coincident and the grid cell includes the coastal strip [12–13°E; 44–45°N] up to approximately the 40 m bathymetric (red square in Figure 1b). The ERSST grid cell (blue square in Figure 1b) is wider than the others, due to its coarser resolution and it encloses a central area of the Northern Adriatic sea [13–15°E; 43–45°N], which does not include the considered coastal strip. The CMEMS SST sea grid points falling inside the HadISST and COBE-SST grid cell have been selected from daily fields to compute monthly averages and represent the best SST estimate of the coastal area under investigation.

237 A preliminary consistency analysis of the monthly SST time series has been conducted and is provided
238 in the supporting information (Figure S1). The outcome suggests a consistency among the centennial SST data
239 sets and CMEMS SST and their potential usability to characterize the long term SST variations of the domain
240 under investigation.

241 SST annual averages and relative anomalies have been computed subtracting from each time series its
242 relative time average (i.e. 1900-2014 for the centennial datasets, 1982-2018 for CMEMS SST). The resulting
243 annual SST anomalies are displayed in Figure 3 together with the annual RSL values from Cerenzia et al.,
244 (2016).

245 The correlation between the annual anomalies from the centennial SST datasets and the reference
246 CMEMS SST have been computed over the time period 1982–2018 in order to select the most correlated one to
247 be used in the successive multivariate analysis. The correlation is highly significant and it is equal to 0.85 for
248 COBE-SST, 0.86 for HadISST and 0.88 for ERSST. The correlation among all four SST annual anomalies and
249 the annual RSL has been computed too and it results minimum for COBE-SST (0.42) and maximum for
250 CMEMS SST (0.63), while it is equal to 0.54 and 0.55 for HadISST and ERSST respectively.

251 The analysis of the available centennial datasets suggested to select the ERSST annual averages for the
252 successive analyses on sediment OM data due to its highest correlation with both CMEMS SST and RSL, even
253 if its grid mesh does not include the area under investigation (Figure 1). The reason could depend from the
254 largest availability of in situ data within the ERSST widest grid box on which the gridded data product relies,
255 making its estimate more robust.

256

257 2.5 Multivariate statistical analysis

258 The constrained ordination method of redundancy Analysis (RDA, Legendre and Legendre, 2012) was
259 employed to evaluate the relation between sediment OM data (response variables) and the climatic ERSST and
260 RSL data (explanatory variables). The analysis was carried out using the R package VEGAN. The overall
261 significance of the RDA model and of the single explanatory variables was tested using the `permutest()` and
262 `anova.rda()` functions of VEGAN, which are based on permutation methods. Due to the availability of RSL and
263 SST data, the period prior to 1897 and the periods 1922–1935, 1941–1945 and 1990–1994 could not be
264 included in the RDA. Organic matter data and climatic variables were further averaged during the period
265 comprised by each core section. Four distinct RDA were performed, one for each core. Correlation between
266 single explanatory and response variables and between variables and RDA axes was quantified and tested using
267 the Pearson's r coefficient.

268

269 3 Results

270 3.1 ^{210}Pb geochronology

271 The excess ^{210}Pb profile showed a decreasing trend with depth, and activities ranged from 0.8 to 33.5 Bq
272 kg^{-1} in the saltmarsh habitat, and from 14.4 to 58.7 Bq kg^{-1} in the impacted habitat, with an overall mean value
273 of 23.1 ± 17.0 Bq kg^{-1} . The period covered by each sedimentary core is longer than 100 years, and the time span
274 from 1900 to 2008 (Figure S2). The average sediment accumulation rates (SAR, 0.15 ± 0.06 cm yr^{-1} and
275 0.21 ± 0.06 cm yr^{-1}) and mass accumulation rate (MAR, 0.16 ± 0.07 and 0.17 ± 0.06 $\text{g cm}^{-2} \text{yr}^{-1}$) were comparable
276 in the saltmarsh habitat and the impacted habitat, respectively.

277 The modern (last decades to century) sediment chronologies estimated from the excess ^{210}Pb CF-CS
278 model were compared to the profiles of THg concentration (Table S1). Generally, the THg concentration
279 increased from low near background regional values in the bottom layers to the maximum values in the sub-
280 surface layers followed by a rapid decrease towards the upper layers (Figure S3). THg concentrations were
281 < 0.12 mg kg^{-1} up to 9 cm and 12 cm depth in the saltmarsh and impacted habitat cores, respectively (1950±4

and 1953±4). The onset of THg was recorded in the middle layers of the impacted habitat core and the saltmarsh habitat core (11 and 8 cm, respectively; year 1957±3). The highest values of THg were found in the middle layers of the impacted habitat core (6–9 cm, from year 1967±3 to 1977±2), where the concentrations of THg were always higher than 20 mg kg⁻¹, with a maximum value of 25.3 mg kg⁻¹ (7 cm, year 1977±2).

The mean differences of geochronology (1958 and 1978) between the results from excess ²¹⁰Pb and THg are 1.0±0.7 years and 2.5±5.1 years, respectively. The relatively consistent estimation results of ²¹⁰Pb and THg indicated the geochronology was valid, although the biggest uncertainty (6.1 years) was found in the saltmarsh core (Table S1).

3.2 Elemental and isotopic composition of sedimentary organic carbon

The OC content, C/N ratio and δ¹³C in the surface sediment ranged from 1.04 to 2.62%, from 6.92 to 10.99, and from -21.87 to -18.21‰ in the saltmarsh habitat, and from 0.68 to 2.62%, from 6.98 to 11.1, and from -26.81 to -20.91‰ in the impacted habitat (Table S2). δ¹³C values were significantly enriched in the saltmarsh habitat when compared to the impacted habitat (-20.06±1.31 ‰ and -23.34±2.00 ‰; p < 0.007), whereas C/N ratios did not show any significant difference between the surface sediments from the saltmarsh and impacted habitats.

On the basis of ²¹⁰Pb chronology and historical Hg concentrations, three time periods were defined: before 1957, 1957–1977, and after 1977.

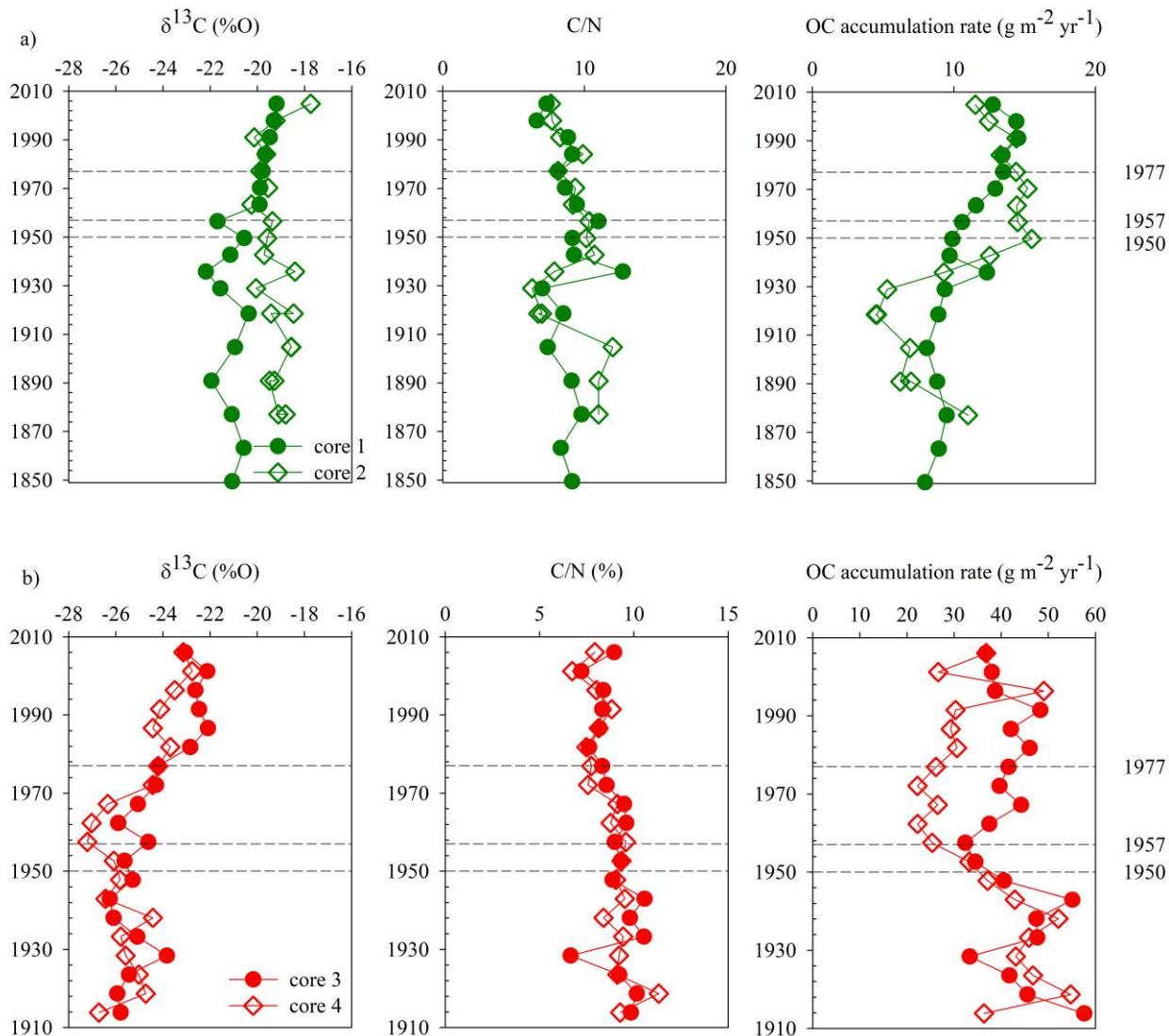
In the saltmarsh habitat cores, OC content ranged from 0.38 to 1.38% and from 0.22 to 1.31% (core 1 and core 2), and from 2.06 to 3.74% and from 2.53 to 3.94% in the impacted habitat cores (core 3 and core 4); C/N ratio varied from 6.62 to 12.73 and from 6.32 to 15.80 in the saltmarsh habitat (core 1 and core 2), and from 6.64 to 10.56 and 6.74 to 11.33 in the impacted habitat (core 3 and core 4). The range of variation of δ¹³C was -22.19 to -19.19 ‰ and -20.25 to -17.74 ‰ in the saltmarsh habitat (core 1 and core 2, respectively), and -26.26 to -22.09 ‰ and -27.21 to 22.76 ‰ in the impacted habitat (core 3 and core 4, respectively) (Figure 2 and Table S3).

In the saltmarsh habitat, δ¹³C values were slightly but significantly depleted in the sediments deposited before the 1950s than in recent years (1980s–2008) (-21.15±0.60 ‰ and -19.41±0.21 ‰, p < 0.001) in core 1; conversely, core 2 did not display any significant difference over time (-19.12±0.55 ‰ and -19.18±1.03 ‰, respectively). In the impacted habitat, δ¹³C values in recent sediments (-22.54±0.39 ‰ in core 3 and -23.61±0.62 ‰ in core 4) displayed a marked and significant enrichment in comparison to the 1960s–1970s intermediate layers (-24.82±0.69 ‰, p < 0.001 in core 3, and -25.84±1.43 ‰, p = 0.003 in core 4) and older layers deposited prior to the 1950s (-25.49±0.73 ‰, p < 0.001 in core 3 and -25.62±0.77 ‰, p = 0.002 in core 4).

In the saltmarsh habitat, C/N ratios did not display any significant increase from recent sediments (1980s–2008) to the older layers deposited prior to the 1950s in core 1 (7.98±1.20 and 9.04±1.56) and in core 2 (8.38±1.05 and 9.71±3.47). In the impacted habitat, C/N ratios slightly but significantly increased from recent sediments (1980s–2008) to the older layers deposited prior to the 1950s both in core 3 (8.11±0.61 and 9.44±1.20, respectively; p = 0.038) and core 4 (7.85±0.70 and 9.41±0.79, respectively; p = 0.004).

Accumulation rates of OC ranged from 8.0 to 14.6 g m⁻² yr⁻¹ and 4.5 to 15.5 g m⁻² yr⁻¹ in the saltmarsh habitat (core 1 and core 2), and from 32.4 to 57.6 g m⁻² yr⁻¹, and 22.2 to 54.7 g m⁻² yr⁻¹ in the impacted habitat (core 3 and core 4). In the saltmarsh habitat, OC accumulation rates were slightly but significantly higher in intermediate and recent sediments (1960s–2008) than in the older layers deposited prior to the 1950s both in core 1 (12.97±1.35 g m⁻² yr⁻¹ and 9.35±1.23 g m⁻² yr⁻¹, respectively; p = 0.003) and in core 2 (13.79±1.25 and 8.40±3.69 g m⁻² yr⁻¹, respectively; p = 0.047). In the impacted habitat, there were no significant differences in OC accumulation rates between the older, intermediate and recent layers in core 3 (44.82±8.30, 39.04±4.48, and 41.63±4.68 g m⁻² yr⁻¹, respectively). In core 4, OC accumulation rates were significantly higher in the older

328 layers deposited prior to the 1950s than in intermediate (1960s–1970s) and recent sediments (1980s–2008)
 329 (43.57 ± 7.20 , 24.51 ± 2.11 , and 33.78 ± 8.20 $\text{g m}^{-2} \text{yr}^{-1}$; $p < 0.001$ and $p = 0.034$, respectively) (Figure 2).



330

331

332 Figure 2. Vertical distributions of stable carbon isotope ($\delta^{13}\text{C}$), C/N ratio, and OC accumulation rates in recent
 333 deposited sediments (1978–2008), intermediate layers (1957–1977) and older layers (deposited prior to the
 334 1950s) within Pialassa Baiona coastal lagoon from a) the saltmarsh habitat and b) the impacted habitat.

335

336

3.3 Climatic site characterization

337 The RSL time series over the considered 1900–2014 time period (Figure 3) is characterized by a total
 338 variation of 98.4 cm with a continuous rise starting from the '40s until present, characterized by a steep increase
 339 from the '40s to the '70s. The RSL trend is equal to 8.7 ± 0.5 mm yr^{-1} , which reduces to 7.0 ± 1.4 mm yr^{-1} in the
 340 most recent 1982–2014 time period.

341 Cerenzia et al. (2016) highlight the dominant role of land movement on the RSL rise in this area and
 342 report a natural subsidence trend of about 6 mm yr^{-1} in the time period 1897–1950 followed by a noticeable
 343 increase over the period 1950–1970, corresponding to a rate of about 24 mm yr^{-1} . Bruni et al., (2019) also

describe a moderate RSL rising tendency before 1940, a steep increase from the '40 to the 70s and its significant reduction after 1980.

The effect of human activities in the study area is thus predominant in the area with respect to SL rise, especially from the '40s until the 1970s, when subsidence due to groundwater withdrawal from surface aquifers and gas extraction have superimposed onto the regional tectonic component. As a consequence the sea water ingress within the coastal lagoon increased in time, modulated by tidal flow.

SST annual anomalies (Figure 3) appear mainly negative during the first two decades (1900–1920), they fluctuate approximately between $\pm 0.5^\circ\text{C}$ from 1920 to 1970 with the most pronounced ERSST negative anomalies during the 1940s. Between 1970 and the early 1980s the anomalies become mainly positive, but since that period the SST start a continuous warming tendency characterized by always positive anomalies approximately after the year 2000. Consistently, CMEMS SST anomalies appear mostly negative before the year 2000 and positive afterwards.

The total ERSST variation over the 1900–2018 time period is equal to 1.0°C with a constant increase of $0.009 \pm 0.002^\circ\text{C yr}^{-1}$. SST increases mainly from the early 1980s, thus the linear trends in the time period 1982–2018 is provided too: ERSST trend is equal to $0.034 \pm 0.010^\circ\text{C yr}^{-1}$ and CMEMS SST is $0.044 \pm 0.009^\circ\text{C yr}^{-1}$. The latest value is comprised within the estimates by Pisano et al. (2020) for the whole Mediterranean Sea ($0.041 \pm 0.006^\circ\text{C yr}^{-1}$) and the Adriatic Sea ($0.045 \pm 0.007^\circ\text{C yr}^{-1}$).

Starting from the '80s the effect of subsidence slowed down due to mitigation effects but SL rise continues at a rate of about $2.2 \text{ mm} \pm 1.3 \text{ mm yr}^{-1}$ (1990–2011; Cerenzia et al., 2016) and contemporary SST increases with unprecedented rate.

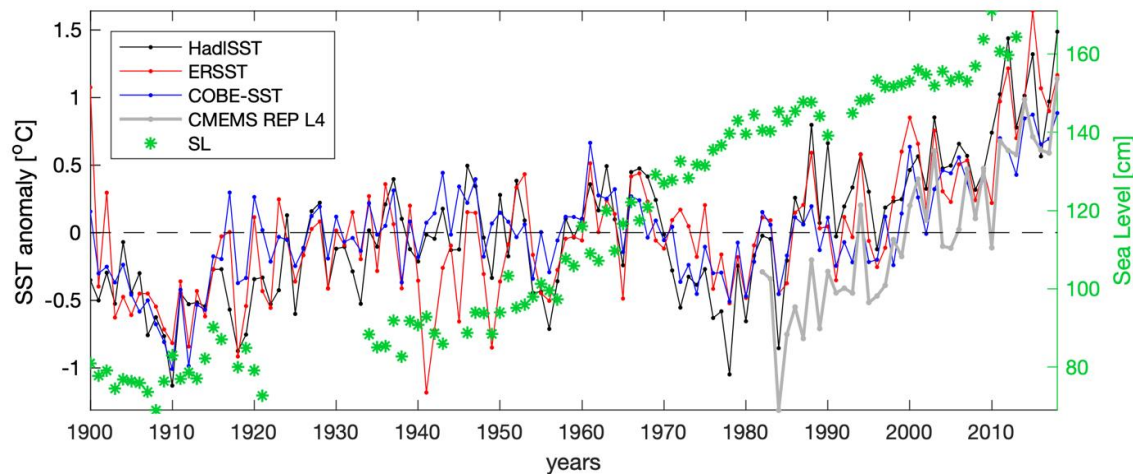


Figure 3. Annual mean time series of RSL (1900–2014) at the Porto Corsini tide gauge (Cerenzia et al., 2016) and SST anomalies (1900–2018) from three global data products (HadISST, ERSST, COBE-SST) and a reference regional data product from CMEMS (1982–2018). SST data products characteristics are summarized in Table 1.

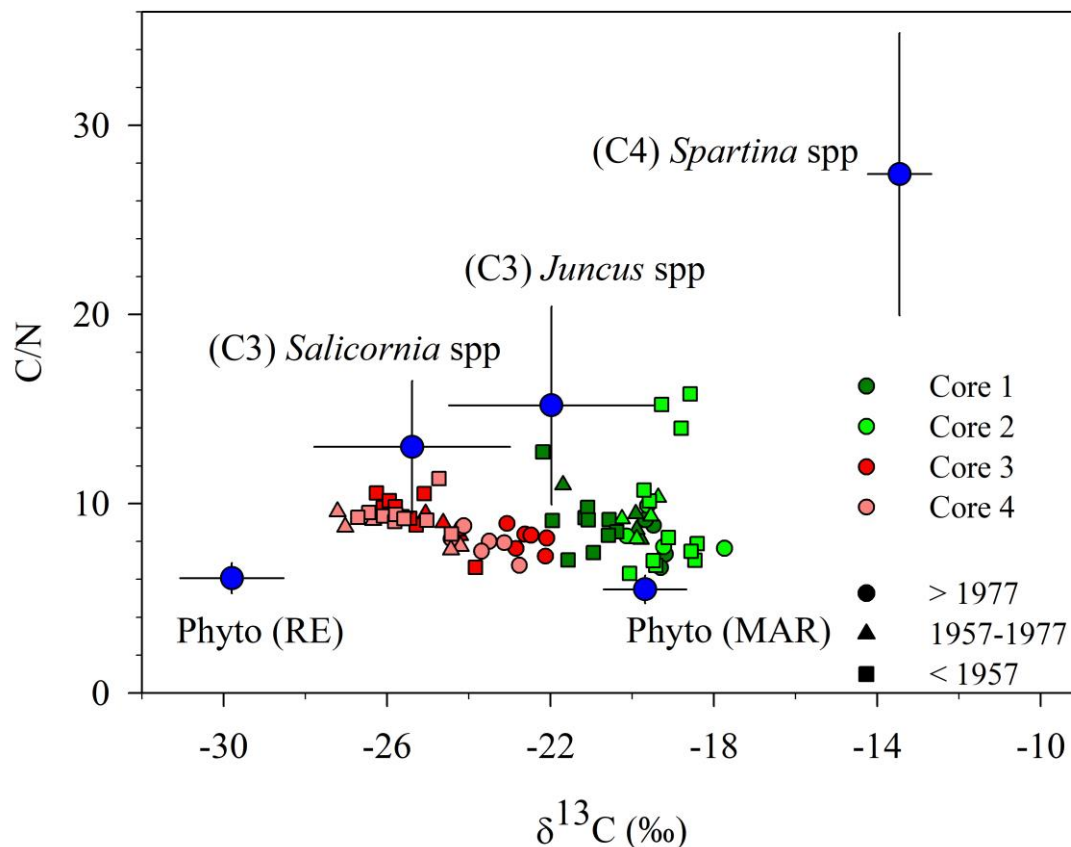
4 Discussion

4.1 Organic matter sources

Coastal wetlands ecosystems represent the convergence of terrestrial and marine systems, hence stable carbon isotopes ($\delta^{13}\text{C}$) and the ratio of organic carbon to total nitrogen (C/N) values of these environments will

375 depend on the relative contributions of carbon derived from saltmarsh vascular vegetation, phytoplankton,
 376 seagrasses, algae, and particulate organic carbon (POC) transported by rivers and tides (Lamb et al., 2006). $\delta^{13}\text{C}$
 377 and C/N together are able to differentiate sources of OM that accumulate in coastal depositional records,
 378 specifically between C3 and C4 vegetation and freshwater and marine organic matter (Kemp et al., 2012, 2010;
 379 Khan et al., 2015b; Oreska et al., 2018).

380 In order to estimate the relative contribution of different OM sources supplied to and stored in sediments
 381 of Pialassa Baiona coastal lagoon, we combined $\delta^{13}\text{C}$ and C/N values of saltmarsh habitat cores ($n = 38$),
 382 impacted habitat cores ($n = 40$), and saltmarsh and impacted habitat surface sediments ($n = 6$ and $n = 6$,
 383 respectively) (Table S2 and S3 in the supporting information). The $\delta^{13}\text{C}$, C/N and OC composition of modern
 384 sediments (c.a. last century) in the two habitats of the lagoon generally indicated their spatial and temporal
 385 distribution (Figure 3 and Figure 4). Despite this distinct pattern, a significant positive correlation ($p < 0.0001$, n
 386 $= 88$) between contents of OC and TN was observed with a strong linear relationship and a close to zero
 387 intercept ($\text{TN} = 0.01312 \cdot \text{OC} + 0.0048$; $r^2 = 0.9459$). This clearly indicates common OM sources in the two
 388 habitats, and suggests that nitrogen in sediments was predominantly bound to sedimentary OC, thus is probably
 389 in an organic form (Hedges et al., 1986).



390

391 Figure 4. Plot of the stable OC isotopic compositions ($\delta^{13}\text{C}$) and atomic carbon: nitrogen ratios (C/N) in recent
 392 deposited sediments (1980s–2008), intermediate layers (1960s–1980s) and older layers (prior to the 1950s)
 393 from the saltmarsh habitat (core 1 and core 2) and the impacted habitat (core 3 and core 4) within Pialassa
 394 Baiona coastal lagoon (Gebrehiwet et al., 2008; Guerra et al., 2013; Hughes and Sherr, 1983; Kelleway et al.,
 395 2017; Kemp et al., 2012, 2010; Lamb et al., 2006). The compositions of five possible OM sources: marsh (C3)
 396 vascular vegetation (*Juncus* spp. and *Salicornia* spp.), marsh (C4) *Spartina* spp., riverine-estuarine
 397 phytoplankton (Phyto (RE)), marine phytoplankton (Phyto (MAR)), are plotted to show the relative contribution
 398 of allochthonous and autochthonous OM.

399

The C/N ratio has been used as effective index to characterize predominant sources of OM in coastal marshes and lagoons (Cloern et al., 2002; Khan et al., 2015b; Meyers, 1994; Wilson, 2017). Previous studies reported C/N ratios for C3 and C4 saltmarsh vegetation OM that are typically >12, whereas values for marine OM are <8; intermediate values are thought to be mixed. C/N values varies little between the saltmarsh and impacted habitats sediments and is consistently <10 with very few exceptions (Figure 3 and Figure 4). The C/N ratio indicates that the sedimentary OM in the saltmarsh and impacted habitats had a mixed source of freshwater- and marine-derived OM, and the freshwater source of OM was mainly distributed in the impacted habitat, while the saltmarsh habitat was dominated by marine source OM. Despite the overall low C/N values, still a slight but consistent increasing trend from recent layers (1980s–2008) to the pre 1950s sediments can be identified in the impacted habitat (Figure 3b). Significant changes in C/N typically occur in early stages of OM microbial degradation (Dai et al., 2005), and this may have resulted in in situ lower surface sediment C/N compared to the older deposited layers.

Carbon isotope signatures clearly allocated sediments in two distinct groups, with enriched $\delta^{13}\text{C}$ values found in the saltmarsh habitat, and relatively depleted $\delta^{13}\text{C}$ values in the impacted habitat lying between values for corresponding marine and riverine-estuarine end-members (Figure 4). These $\delta^{13}\text{C}$ values infer a change in OM sources from the saltmarsh to the impacted habitat, and reflect contributions from mixed sources of sedimentary OM suggesting that allochthonous freshwater/riverine sources may have a local influence in the impacted habitat, while allochthonous marine sources seem to predominate in the saltmarsh habitat. The $\delta^{13}\text{C}$ values of the saltmarsh and impacted habitats partially overlay the isotopic signatures of saltmarsh vegetation of a C3 photosynthetic pathway origin, which have a $\delta^{13}\text{C}$ extent of -29.88 to -20.2 ‰ and a C/N of 9.70 to >20 (Khan et al., 2015a; Lamb et al., 2006). So far C4 saltmarsh plants are either absent or have been recently introduced in North European saltmarshes (Preston et al., 2002); to our knowledge there is no record of C4 *Spartina* spp. presence in Pialassa Baiona coastal lagoon in the scientific and grey literature.

Locally produced (autochthonous) biomass is generally considered to contribute significantly to the total OC pool in saltmarsh sediments (Chen et al., 2016). Among saltmarsh vascular vegetation, species of the genus *Juncus* is the prevailing C3 high marsh plant of Pialassa Baiona coastal lagoon (Merloni and Piccoli, 1999). Allochthonous sources are the marine-derived OM, imported through tidal flow from the main channel connecting to the sea, and the riverine-estuarine derived OM, brought in by the main inflow channel located on the southern edge of the lagoon, while *Juncus*-derived OM is likely produced in situ, and thus represents an autochthonous source in the sedimentary OM of the saltmarsh and impacted habitats.

To estimate the proportional contribution of the different sources to the sediment OM in each of the cores we applied MixSIAR, a Bayesian mixing model framework implemented as an open-source R package (Stock et al, 2018). MixSIAR, and mixing models in general, require tracer data that characterize the chemical or physical traits of both the sources and the mixtures; these traits are assumed to predictably transfer from sources to mixtures through a mixing process. In the present application $\delta^{13}\text{C}$ and C/N are used as tracers. Marine phytoplankton, riverine/estuarine phytoplankton and *Juncus* spp. are considered the potential sources while sediments are the mixtures.

Tracer values for marine phytoplankton ($\delta^{13}\text{C}$: -19.7 ± 1.0 ‰; C/N: 5.5 ± 0.7) and for riverine/estuarine phytoplankton ($\delta^{13}\text{C}$: -29.8 ± 1.3 ‰; C/N: 6.1 ± 0.8) were obtained from Tesi et al. (2007) and Guerra et al. (2013). Values for *Juncus* spp. ($\delta^{13}\text{C}$: -22.0 ± 2.5 ‰; C/N: 15.2 ± 5.2) were obtained from Gebrehiwet et al. (2008) and Kelleway et al. (2017).

Regardless of the tracers or mixing system considered, all mixing model applications are rooted in the same fundamental mixing equation:

$$Y_j = \sum_k p_k \mu_{jk}^s$$

where the mixture tracer value, Y_j , for each of j tracers is equal to the sum of the k source tracer means, μ_{jk}^s , multiplied by their proportional contribution to the mixture, p_k .

MixSIAR, through the application of Markov chains Monte Carlo sampling, estimates the probability density function of each pk value, i.e. the proportional contribution of each source to the final mixture. Statistics like mean and standard deviation are then calculated from this estimated distribution. Bayesian mixing models improve upon simpler linear mixing models by explicitly taking into account uncertainty in source values. MixSIAR, in particular, has the ability to incorporate categorical and continuous covariates to explain variability in the mixture proportions and offers several options for error parametrization.

In our analysis, two categorical covariates, core and time period, were taken into account. Error was assumed as “residual only”, in accordance with the indications of Stock et al. (2016) for the application of mixing models to sediment sourcing. The probability density functions of the proportional contributions of the three sources to the sediment OM are shown in Figure S4, separately for each core and time period. Means, standard deviations and percentiles of the same distributions are reported in Table S4.

The marine-derived OM increased from ~50% in the sediments deposited prior to the 1950s to ~70% in recent decades (1980s–2008) in the saltmarsh habitat. Similarly, marine-derived OM increased from ~15% in the sediments deposited prior to the 1950s to ~40% in recent decades (1980s–2008) in the impacted habitat. Riverine-estuarine OM sources accounted for <10% and ~50 % of sedimentary OM in the saltmarsh and impacted habitats over the last century; these sources decreased from ~60% in the pre 1950s period to ~40% in recent decades (1980s–2008), while marine-derived OM contribution increased simultaneously after the 1950s within the impacted habitat. These findings indicate that the relative contribution of marine-derived OM to recent sediments are larger than in sediments deposited prior to the 1950s, and this contribution is by ~30% higher in saltmarsh habitat sediments than in the impacted habitat. The explanation of the increasing contribution of tidally-derived OM is related to an increasing inflow of sea water into the lagoon over the last decades supported by the positive RSL trend recorded by the tide gauge.

$\delta^{13}\text{C}$ signatures and C/N showed that an important fraction of sedimentary OM stored in sediment within Pialassa Baiona coastal lagoon is derived from the autochthonous C3 saltmarsh plant *Juncus* spp. Overall, this fraction is slightly higher within the saltmarsh habitat, where C3 saltmarsh vegetation-derived OM comprised on average ~33% of the OM sedimentary pool when compared to the ~26% fraction in the impacted habitat sediments. The mixing model evidenced a change in C3 saltmarsh vegetation OM contribution from ~40% to ~20% in the sediment records from the saltmarsh habitat in the pre 1950s period to recent decades (1980s–2008) concomitant with the increased marine-derived OM contribution from the 1950s forward, and from ~30 to ~25% in the impacted habitat, respectively. The most plausible explanation is that $\delta^{13}\text{C}$, OC and C/N geochemistry of sediments varied in relation to mixing of the autochthonous OM from in situ C3 saltmarsh vegetation with an increased contribution from allochthonous particulate OM from marine sources, which in turn, is controlled primarily by tidal inundation.

4.2 Relationship between organic matter and climatic variables

Redundancy analysis (RDA) was employed to determine if the observed spatial and temporal variability in sedimentary OM data was related to regional climatic changes (Figure 5). RDA model, tested by using the permutest procedure, is highly significant for all the cores except core 2 (Figure 5b). RDA axes account from 38% (core 4) to 66% (core 1) of the total variation, thus a large fraction of the differences in sediment OM properties among core sections is not explained by the RSL and SST (Figure 5, Table S5). The first axis (RDA1) accounts for 86% (core 3) to 97% (core 1) of the explained variance and was positively correlated with both RSL and SST, although RSL had higher scores on this axis. The second axis (RDA2), which accounts only for 3% to 14% of explained variance, was mostly related to SST. As a consequence, RDA1 can be interpreted as the conjunct variation of RSL and SST, while RDA2 as the fraction of SST variation that is not related to the RSL. However, SST presents little independent explanatory power since its effect, tested using the anova.rda procedure, is in all cases not significant. On the other hand the effect of RSL is highly significant in the three cores (1, 3 and 4) where the RDA model is also highly significant.

492 Recent years (after 1977) show high values on RDA1 axis (except for core 2 not significant) well
493 separated from older years (before 1957), which are instead characterized by low values. Years 1957–1977
494 score intermediate values and overlap with both recent and older years. This result reflects the steady rise in
495 RSL and SST changes over the last century (Figure 3): low RDA1 scores before 1957 when both RSL and SST
496 rise are low, intermediate RDA1 scores between 1957 and 1977 when SST is not increasing while RSL rapidly
497 increases mainly under the effect of subsidence, while high RDA1 scores appear after 1977 when both RSL and
498 SST increase.

499 TN was positively correlated with RDA1 and C/N ratio was negatively correlated with RDA1 in all four
500 cores. On the other hand, the relation between other OM variables and RDA1 was not consistent among the four
501 cores. OC content was positively correlated with RDA1 and TN content in the saltmarsh habitat (cores 1 and 2),
502 while independent from RDA1 in the impacted habitat (cores 3 and 4). Correlation between OC accumulation
503 rate and RDA1 was positive in the saltmarsh habitat, negative in the impacted habitat, although correlation was
504 significant only for cores 1 and 4. $\delta^{13}\text{C}$ was positively correlated with RDA1 in all cores with the exception on
505 core 2 (saltmarsh habitat).

506 In summary RDA suggested that climatic variables, in particular RSL due to the cumulated effect of
507 land movement and SL rise, influenced OM properties of the sediments. However, the effect of this influence
508 was not consistent between the two habitats, and differences were observed even between cores from the same
509 habitat.

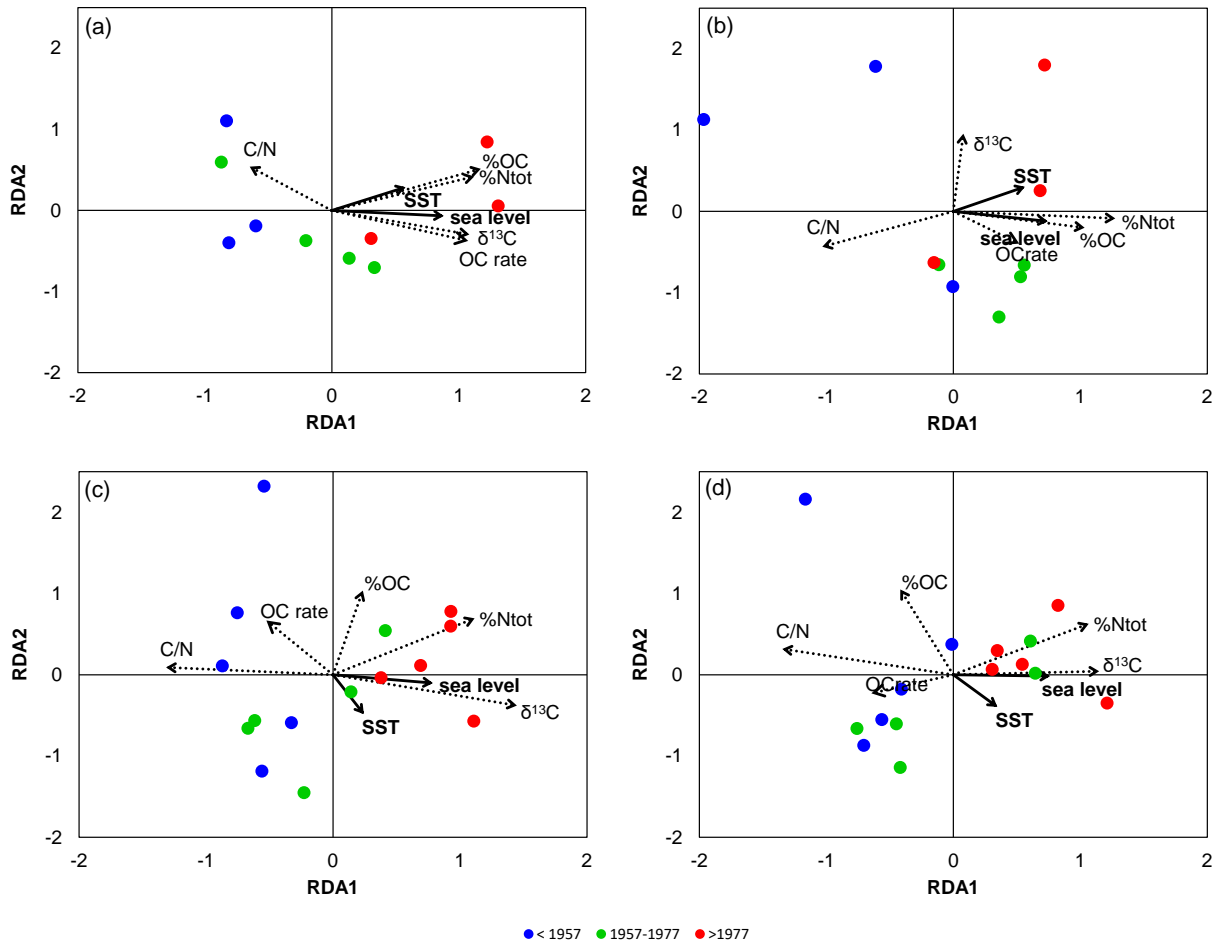


Figure 5. Plot of RDA analysis with response sedimentary OM variables (OC, $\delta^{13}\text{C}$, OC accumulation rates) and explanatory regional climatic variables (RSL and SST): (a) saltmarsh habitat core 1, (b) saltmarsh habitat core 2, (c) impacted habitat core 3 and (d) impacted habitat core 4.

4.3 Organic matter accumulation

Core dating using excess ^{210}Pb confirmed that the sediment bed has accreted due to sediment accumulation in the saltmarsh and impacted habitats over the last century. The differences in geochronology resulting from excess ^{210}Pb and THg can be attributed to complex depositional conditions and biogeochemical cycling with northward migration of Hg causing a delayed THg peak (Covelli et al., 2011; Fabbri et al., 2001; Trombini et al., 2003).

Pb-210 derived SARs are comparable with published accretion rates measured within Oregon tidal saline wetlands ($0.13\text{--}0.29\text{ cm yr}^{-1}$) and Long Island Sound ($0.1\text{--}0.36\text{ cm yr}^{-1}$) (Peck et al., 2020; Hill and Anisfeld, 2015), in microtidal coastal wetlands in the Gulf of California and the Caribbean Sea ($0.04\text{--}0.65\text{ cm yr}^{-1}$) (Ruiz-fernández et al., 2018), and within Venice lagoon under rising sea level, subsidence and increasing frequency of high tides flooding called ‘acqua alta’ ($0.13\text{--}0.44\text{ cm yr}^{-1}$) (Bellucci et al., 2007).

Salt marshes are vulnerable and dynamic systems that can extend landward in response to lateral erosion and accrete vertically by accumulating sufficient materials to compensate for rising sea level (Fagherazzi et al., 2020; Kirwan and Megonigal, 2013; Mariotti and Carr, 2014). Sediment accretion is further promoted by the presence of halophytic plants producing OM, which in turn, can be partially buried favoring net sediment accumulation (Cahoon et al., 2021).

531 To explore whether Pialassa Baiona lagoon is a net depositional or erosional area, excess ^{210}Pb (Bq
532 cm^{-2}) inventories were estimated at sediment core habitats according to a standard technique (Appleby and
533 Oldfield, 1992), and then compared to the annual atmospheric flux of ^{210}Pb within the latitudinal range 40–50°N
534 ($0.0155 \pm 0.0075 \text{ Bq cm}^{-2} \text{ yr}^{-1}$) (Baskaran, 2011). The mean excess ^{210}Pb inventory for sediment cores at the
535 saltmarsh and impacted habitats is $0.37 \pm 0.27 \text{ Bq cm}^{-2}$, which is lower than the steady state inventory of
536 atmospheric ^{210}Pb ($0.50 \pm 0.24 \text{ Bq cm}^{-2}$) at 40–50°N, and thus the study area is not net depositional.

537 Averaged SAR over the period ~1900–2010 ($\sim 0.2 \text{ mm yr}^{-1}$) is lower than the local RSL (Cerenzia et al.,
538 2016) increase owing to rapid land subsidence in the 1950–1970, thus indicating the accretion balance is
539 negative and the area is less likely to keep pace with the ongoing SL rise. SL rise scenarios for the year 2100
540 and relative inundations map for the subsiding Northern Adriatic coastal plain, predict that the coastal area
541 under investigation will be most probably submerged by that time (Antonioli et al., 2017; Mariano et al., 2021).

542 Although OC accumulation rates averaged over 1900s–2008 are lower than the averages for tidal
543 wetlands soils and salt marsh sediments (Ouyang and Lee, 2014; Wang et al., 2019), they compare well to mean
544 OC rate in modern sediments (ca < 200 yrs) in coastal and inland aquatic ecosystems (Wilkinson et al., 2018). In
545 terms of carbon sequestration, our data suggests that modern sediments in the study area are similar to recently
546 deposited sediments soils in vegetated U.K. salt marsh habitats, as well as salt marshes in the Blackwater,
547 Sheldth, and Guadiana estuaries (Table 2).

548 The variation of modern OC accumulation rates between the two habitats is remarkable, with the highest
549 values found in the impacted habitat located in the southern lagoon, an area that historically received
550 allochthonous inputs of OC and nutrients from agriculture runoff and wastewater discharges through the main
551 inflow channel draining an intensely cultivated watershed (Giordani et al., 2005). Lower OC values were found
552 in the saltmarsh habitat located in the northern area of the lagoon, distal from the main freshwater and anthropic
553 inputs from inland activities.

554 Before the 1950s, OC accumulation rates in the impacted habitat were on average higher and negatively
555 correlated with RSL, a trend confirmed as statistically significant for core 3. This could be explained by a
556 decrease in the amount of suspended solids entering the inflow channels from the watershed. While there are no
557 direct measurements available for the time period under consideration, this appears to be in line with the
558 recorded hydrological changes in the area (Buscaroli et al., 2011).

559 In the nineteenth century, the inland of Pialassa Baiona, which is now entirely reclaimed agricultural
560 land, was predominantly formed up of wetlands, which were connected to the lagoon through channels. The
561 Lamone River, which previously flowed directly into the Adriatic Sea north of Pialassa Baiona, was redirected
562 to flow into the wetlands southwest of the lagoon in 1846, to reclaim agricultural land by filling the wetlands
563 with sediments brought by the river. When the southern wetlands were filled, the river was shifted northward,
564 finally returning to run directly into the Adriatic Sea north of Pialassa Baiona at the turn of the 1950s. As a
565 result of the reclamation process, the lagoon was gradually cut off from the Lamone river's suspended solids
566 flow.

567 Our hypothesis is that the balance between increasing sedimentation of marine OM (due to RSL rise)
568 and decreasing riverine OM was somewhat negative in the impacted habitat, resulting in a decrease in OC
569 accumulation rate over time. Conversely, the saltmarsh habitat was already excluded from riverine OM
570 contributions at the turn of the nineteenth century, and thus increased sedimentation of marine OM resulted in
571 an increase of OC accumulation rate.

572 A plausible explanation of the lower OC accumulation rates found in this habitat could be attributed to
573 the predominance of marine phytoplankton sources increasing with RSL rise over the last century with a minor
574 contribution from prevailing C3 saltmarsh vegetation (*Juncus* spp.) as evidenced by the isotopic ^{13}C signals and
575 the MixSIAR model outputs. Marine phytoplankton predominantly consists of macromolecules (pigments,
576 lipids, carbohydrates, and aminoacids) that show a steady decline through the water column into the sediments
577 (Hama et al., 2004; Wakeham et al., 1997) in contrast to intrinsically refractory components (for example lignin
578 and lipid biomarkers) typical of terrestrial angiosperms (Hedges and Mann, 1979), and of marine and wetland

579 vascular plants including *Juncus* spp (Clifford et al., 1995; Goñi and Thomas, 2000; Klap et al., 2000) that are
580 selectively preserved and accumulated into the sedimentary OC pool of coastal systems (Bianchi et al., 2018;
581 Goñi et al., 1998; Kuzyk et al., 2008; Tanner et al., 2010, 2007).

582 OC storage and sink capacity of blue carbon ecosystems, including saltmarshes, are impacted at spatial
583 and temporal scales by rapidly changing climate and anthropogenic factors, comprising SL rise, land
584 subsidence, warming, hydrological alterations, and landscape development (Ouyang and Lee, 2014; Tan et al.,
585 2020), and these disturbances resulted in estimated areal losses of 0.2–7% yr⁻¹ at global level (Spivak et al.,
586 2019). Human-caused and climatic changes have also affected the physical environment of the Pialassa Baiona
587 coastal lagoon and its adjacent areas throughout the previous century, particularly in the middle of the 1900s
588 due to the combination of SL rise and fast subsidence rate, resulting in changes in OM accumulation and
589 sources in their sediments.

591 4.4 Carbon stock

592 For the 1900–2008 period, the carbon stock estimated from the OC accumulation rates is 1253±12 g C
593 m⁻² for the saltmarsh habitat, and 4223±40 g C m⁻² for the impacted habitat. Overall, the estimated amount of
594 OC stored in the two habitats are 1223±24 g C m⁻² and 3800±20 g C m⁻², respectively, of which ~30% are
595 ‘blue carbon’ from in situ C3 saltmarsh vascular vegetation.

596 Between habitat variability has important implications for attempts to characterize blue carbon based on
597 modern environmental conditions (c.a. last century). Our results suggest that contemporary changes in the RSL
598 and allochthonous sources are likely to affect both C stocks and OC accumulation rates. That is, we found
599 approximately threefold differences in OC accumulation rates and C stock between the saltmarsh habitat and
600 the impacted habitat.

601 Over a century scale (1900–2008), the total C pool stored in the sediments is 7379 Mg C and 13682 Mg
602 C in the saltmarsh and impacted habitats (589 ha and 324 ha, respectively), totaling 21061 Mg C corresponding
603 to an area of ~10 km². According to the global dataset of carbon dioxide emissions (World Bank, 2019), Italy
604 per capita CO₂ emissions went from 2.20 in 1960 to 7.11 tons in 2010. If we consider the averaged country’s
605 national CO₂ emissions per capita over this period (6.40 tons), the estimated C pool stored in the two habitats of
606 the Pialassa Baiona amounted to ~77000 Mg CO₂, or the equivalent of ~12000 individuals Italian peoples CO₂
607 emissions per year. These estimates, while small in terms of national CO₂ emissions (338 Mt CO₂;
608 Friedlingstein et al., 2019), are equivalent to 3% of the annual estimated CO₂ emissions from fossil fuel use and
609 combustion of the closest town (Ravenna) (INEMAR-ER, 2019).

611 4 Conclusions

612 OC accumulation rates, OC sources and carbon stock were estimated in ²¹⁰Pb-dated sediment cores from
613 a salt marsh habitat and an impacted habitat within Pialassa Baiona coastal lagoon (Northwestern Adriatic Sea)
614 and paralleled to the temporal trends and changes of SST and RSL in the region. The main findings of this work
615 can be summarized as follows:

- 616 • OC accumulation rates showed a contrasting pattern from the 1950s forward, with a significant
617 increasing trend in the saltmarsh habitat and a decreasing trend in the impacted habitat, though
618 significant only in one core;
- 619 • Allochthonous marine-derived OM sources showed a consistent increase in 1980s–2008 when compared
620 to the pre 1950s period, parallel with a decreased contribution from autochthonous saltmarsh vegetation
621 (*Juncus* spp.) reflecting an increased sea water inflow into the lagoon as confirmed by RSL positive
622 trend in the area;
- 623 • RSL change in the coastal region has been continuously increasing due to the sum of prevailing land
624 subsidence of both natural and anthropogenic origin, and the SL rise. It has been faster during the central
625 decades of the last century, due to the land lowering caused by ground fluids extraction, while it slowed
626 down during the last decades, when subsidence returned to natural rates after the adoption of mitigation
627 measures.
- 628 • SST analysis indicate quite stable SST anomalies until the 1960s, negative anomalies in the 1970s, a
629 rapid and continuous SST increase from the eighties with a trend between $0.034 \pm 0.010^{\circ}\text{C yr}^{-1}$ and
630 $0.044 \pm 0.009^{\circ}\text{C yr}^{-1}$.
- 631 • A direct effect of SST on sedimentary C has not been detected, however RL rise and SST warming are
632 not independent, due to a contribution of thermal expansion to SL rise ranging from 30% to 40%
633 approximately (Storto et al., 2019).
- 634 • Substantial differences have been observed between the saltmarsh and the impacted habitats as to
635 sediment OM composition and sources, rate of accumulation, as well as the temporal trends of these
636 properties and their relationship with climatic variables. Even cores collected few meters apart within
637 the same habitat were appreciably different.
- 638 • The estimated total C pool stored in sediments equals ~3% of the annual estimated CO₂ emissions from
639 the nearby town.

640 The findings of this study confirm that Pialassa Baiona coastal lagoon is an important coastal blue
641 carbon ecosystem in sequestering carbon from atmospheric CO₂ emissions. However, with an annual loss rate
642 of 1–2% between 1980 and 2000 (Spivak et al., 2019) under increasing SL rise and warming, this trend is likely
643 to compromise the capacity of coastal vegetated habitats like Pialassa Baiona coastal lagoon for atmospheric
644 CO₂ uptake and storage, unless proper management and coastal protection is implemented. According to SL
645 rise scenarios and inundations map this coastal vegetated habitat is likely to be submerged by 2100, and thus
646 specific measures should also be implemented to mitigate sea ingression.

647 There are significant data gaps on carbon stocks in coastal vegetated habitats in the Mediterranean
648 Region, and the characteristic variability of these habitats, is a significant challenge to the goal of a global
649 coastal blue carbon inventory. Further research and mapping of C stock and greenhouse gas fluxes including
650 methane (CH₄) in coastal vegetated habitats at regional and national level is strongly recommended.

651 **Acknowledgments and Data**

652 This study was supported by the University of Bologna strategic research grant FinQuer (2007–2009). Mapping,
653 core sampling and handling was graciously conducted by M. Ponti. E. Fetter and S. Righi assisted with
654 laboratory work. We thank Marco Olivieri for providing mean SL data from Cerentia et al. (2016). The
655 Mediterranean Sea Surface CMEMS SST dataset used in this paper is freely distributed through
656 <http://marine.copernicus.eu> and identified as SST_MED_SST_L4_REP_OBSERVATIONS_010_021 in the
657 CMEMS catalogue.

The data sets reported in Table S2 and Table S3 (Supplementary Information) are freely available and accessible at SEANOE, <https://doi.org/10.17882/73534>.

References

- Adams, C.A., Andrews, J.E., Jickells, T., 2012. Nitrous oxide and methane fluxes vs. carbon, nitrogen and phosphorous burial in new intertidal and saltmarsh sediments. *Sci. Total Environ.* 434, 240–251. <https://doi.org/10.1016/j.scitotenv.2011.11.058>
- Airoldi, L., Ponti, M., Abbiati, M., 2016. Conservation challenges in human dominated seascapes : The harbour and coast of Ravenna. *Reg. Stud. Mar. Sci.* 8, 308–318.
- Antolini, G., Auteri, L., Pavan, V., Tomei, F., Tomozeiu, R., Marletto, V., 2016. A daily high-resolution gridded climatic data set for Emilia-Romagna, Italy, during 1961 – 2010. *Int. J. Clim.* 36, 1970–1986. <https://doi.org/10.1002/joc.4473>
- Antonoli, F., Anzidei, M., Amorosi, A., Lo Presti, V., Mastronuzzi, G., Deiana, G., De Falco, G., Fontana, A., Fontolan, G., Lisco, S., Marsico, A., Moretti, M., Orrù, P.E., Sannino, G.M., Serpelloni, E., Vecchio, A., 2017. Sea-level rise and potential drowning of the Italian coastal plains: Flooding risk scenarios for 2100. *Quat. Sci. Rev.* 158, 29–43. <https://doi.org/10.1016/j.quascirev.2016.12.021>
- Appleby, P.G., Oldfield, F., 1992. Application of ²¹⁰Pb to sedimentation studies, in: I. Ivanovich, & R.S.H. (Ed.), *Uranium Series Disequilibrium: Applications to Earth, Marine, and Environmental Sciences*. Oxford University Press, Oxford, pp. 731–778.
- Arriola, J.M., 2017. Variations in carbon burial and sediment accretion along a tidal creek in a Florida salt marsh. *Limnol. Oceanogr.* 62, 2017, 62, S15–S28. <https://doi.org/10.1002/lno.10652>
- Baskaran, M., 2011. Po-210 and Pb-210 as atmospheric tracers and global atmospheric Pb-210 fallout: A Review. *J. Environ. Radioact.* 102, 500–513. <https://doi.org/10.1016/j.jenvrad.2010.10.007>
- Beaumont, N.J., Jones, L., Garbutt, A., Hansom, J.D., Toberman, M., 2014. The value of carbon sequestration and storage in coastal habitats. *Estuar. Coast. Shelf Sci.* 137, 32–40. <https://doi.org/10.1016/j.ecss.2013.11.022>
- Bellucci, L.G., Frignani, M., Cochran, J.K., Albertazzi, S., 2007. Pb and ¹³⁷Cs as chronometers for salt marsh accretion in the Venice Lagoon e links to flooding frequency and climate change 97. <https://doi.org/10.1016/j.jenvrad.2007.03.005>
- Bertoni, W., Brighenti, G., Gambolati, G., Gatto, P., Ricceri, G., Vuillermin, F., 1988. Risultati Degli Studi e Delle Ricerche Sulla Subsidenza di Ravenna. Ravenna.
- Bianchi, T.S., Cui, X., Blair, N.E., Burdige, D.J., Eglinton, T.I., Galy, V., 2018. Centers of organic carbon burial and oxidation at the land-ocean interface. *Org. Geochem.* 115, 138–155. <https://doi.org/10.1016/j.orggeochem.2017.09.008>
- Bonaduce, A., Pardini, N., Oddo, P., Spada, G., Larnicol, G., 2016. Sea-level variability in the Mediterranean Sea from altimetry and tide gauges. *Clim. Dyn.* 47, 2851–2866. <https://doi.org/10.1007/s00382-016-3001-2>
- Boski, A.T., Moura, D., Correia, V., Martins, H., Camacho, S., Journal, S., Issue, S., Proceedings, N., 2021. Postglacial Organic Carbon Accumulation in Coastal Zones - a Possible Cause for Varying Atmospheric CO₂ levels. Preliminary Data from SW Portugal. *J. Coast. Res.* SI 39, 1864–1868.
- Bruni, S., Zerbini, S., Raicich, F., Errico, M., 2019. Rescue of the 1873 – 1922 high and low waters of the Porto Corsini / Marina di Ravenna (northern Adriatic , Italy) tide gauge. *J. Geod.* 93, 1227–1244.
- Buscaroli, A., Dinelli, E., Zannoni, D. 2011. Geohydrological and environmental evolution of the area included among the lower course of the Lamone River and the Adriatic coast. *EQA – Environmental quality / Qualité de l'Environnement / Qualità ambientale*, 5, 11-22.
- Caçador, I., Costa, A.L., Vale, C., 2004. Carbon storage in tagus salt marsh sediments. *Water, Air, Soil Pollut. Focus* 4, 701–714. <https://doi.org/10.1023/B:WAFO.0000028388.84544.ce>
- Cahoon, D.R., McKee, K.L., Morris, J.T., 2021. How Plants Influence Resilience of Salt Marsh and Mangrove Wetlands to Sea-Level Rise. *Estuaries and Coasts* 44, 883–898. <https://doi.org/10.1007/s12237-020-00834-w>
- Calvo-Cubero, J., Ibáñez, C., Rovira, A., Sharpe, P.J., Reyes, E., 2014. Changes in nutrient concentration and carbon accumulation in a mediterranean restored marsh (Ebro Delta, Spain). *Ecol. Eng.* 71, 278–289. <https://doi.org/10.1016/j.ecoleng.2014.07.023>
- Capolupo, M., Franzellitti, S., Kiwan, A., Valbonesi, P., Dinelli, E., Pignotti, E., Birke, M., Fabbri, E., 2017. A comprehensive evaluation of the environmental quality of a coastal lagoon (Ravenna, Italy): Integrating chemical and physiological analyses in mussels as a biomonitoring strategy. *Sci. Total Environ.* 598, 146–159. <https://doi.org/10.1016/j.scitotenv.2017.04.119>
- Carbognin, L., Tosi, L., 2002. Interaction between Climate Changes, Eustacy and Land Subsidence in the North Adriatic Region, Italy 1, 38–50.
- Cerenzia, I., Putero, D., Bonsignore, F., Galassi, G., Olivieri, M., Spada, G., 2016. Historical and recent sea level rise and land subsidence in Marina di Ravenna, northern Italy. *Ann. Geophys.* 59, 1–12. <https://doi.org/10.4401/ag-7022>
- Chen, S., Torres, R., Goñi, M.A., 2016. The Role of Salt Marsh Structure in the Distribution of Surface Sedimentary Organic Matter. *Estuaries and Coasts* 39, 108–122. <https://doi.org/10.1007/s12237-015-9957-z>
- Clifford, D.J., Carson, D.M., McKinney, D.E., Bortiatynski, J.M., Hatcher, P.G., 1995. A new rapid technique for the characterization of lignin in vascular plants: thermochemolysis with tetramethylammonium hydroxide (TMAH). *Org. Geochem.* 23, 169–175. [https://doi.org/10.1016/0146-6380\(94\)00109-E](https://doi.org/10.1016/0146-6380(94)00109-E)
- Cloern, J.E., Canuel, E.A., Harris, D., 2002. Stable carbon and nitrogen isotope composition of aquatic and terrestrial plants of the San Francisco Bay estuarine system. *Limnol. Oceanogr.* 47, 713–729. <https://doi.org/10.4319/lo.2002.47.3.0713>

- 716 Couto, T., Duarte, B., Caçador, I., Baeta, A., Marques, J.C., 2013. Salt marsh plants carbon storage in a temperate Atlantic estuary
717 illustrated by a stable isotopic analysis based approach. *Ecol. Indic.* 32, 305–311. <https://doi.org/10.1016/j.ecolind.2013.04.004>
- 718 Covelli, S., Emili, A., Acquavita, A., 2011. Benthic biogeochemical cycling of mercury in two contaminated northern Adriatic coastal
719 lagoons. *Cont. Shelf Res. J.* 31, 1777–1789. <https://doi.org/10.1016/j.csr.2011.08.005>
- 720 Cuellar-martinez, T., Ruiz-fernández, A.C., Sanchez-cabeza, J., Pérez-bernal, L., Sandoval-gil, J., 2019. Relevance of carbon burial
721 and storage in two contrasting blue carbon ecosystems of a north-east Pacific coastal lagoon. *Sci. Total Environ.* 675, 581–593.
722 <https://doi.org/10.1016/j.scitotenv.2019.03.388>
- 723 Curado, G., Rubio-Casal, A.E., Figueroa, E., Grewell, B.J., Castillo, J.M., 2013. Native plant restoration combats environmental
724 change: Development of carbon and nitrogen sequestration capacity using small cordgrass in European salt marshes. *Environ. Monit.*
725 *Assess.* 185, 8439–8449. <https://doi.org/10.1007/s10661-013-3185-4>
- 726 Cutshall, N.H., Larsen, I.L., Olsen, C.R., 1983. Direct analysis of ^{210}Pb in sediment samples: Self-absorption corrections. *Nuclear*
727 *Instruments and Methods in Physics Research* 206, 309–312.
- 728 Dai, J., Sun, M.Y., Culp, R.A., Noakes, J.E., 2005. Changes in chemical and isotopic signatures of plant materials during degradation:
729 Implication for assessing various organic inputs in estuarine systems. *Geophys. Res. Lett.* 32, 1–4.
730 <https://doi.org/10.1029/2005GL023133>
- 731 Diesing, M., Thorsnes, T., Rún Bjarnadóttir, L., 2021. Organic carbon densities and accumulation rates in surface sediments of the
732 North Sea and Skagerrak. *Biogeosciences* 18, 2139–2160. <https://doi.org/10.5194/bg-18-2139-2021>
- 733 Duarte, C.M., Middelburg, J.J., Caraco, N., 2005. Major role of marine vegetation on the oceanic carbon cycle. *Biogeosciences* 1, 1–8.
734 <https://doi.org/10.5194/bg-2-1-2005>
- 735 Ewers Lewis, C.J., Carnell, P.E., Sanderman, J., Baldock, J.A., Macreadie, P.I., 2018. Variability and Vulnerability of Coastal ‘Blue
736 Carbon’ Stocks: A Case Study from Southeast Australia. *Ecosystems* 21, 263–279. <https://doi.org/10.1007/s10021-017-0150-z>
- 737 Fabbri, D., Vassura, I., Sun, C., Snape, C.E., Mcrae, C., Fallick, A.E., 2003. Source apportionment of polycyclic aromatic
738 hydrocarbons in a coastal lagoon by molecular and isotopic characterisation. *Mar. Chem.* 84, 123–135. [https://doi.org/10.1016/S0304-4203\(03\)00135-X](https://doi.org/10.1016/S0304-4203(03)00135-X)
- 739 Fagherazzi, S., Mariotti, G., Leonardi, N., Canestrelli, A., Nardin, W., Kearney, W.S., 2020. Salt Marsh Dynamics in a Period of
740 Accelerated Sea Level Rise. *J. Geophys. Res. Earth Surf.* 125, 1–31. <https://doi.org/10.1029/2019JF005200>
- 741 Fennessy, M.S., Ibáñez, C., Calvo-Cubero, J., Sharpe, P., Rovira, A., Callaway, J., Caiola, N., 2019. Environmental controls on carbon
742 sequestration, sediment accretion, and elevation change in the Ebro River Delta: Implications for wetland restoration. *Estuar. Coast.*
743 *Shelf Sci.* 222, 32–42. <https://doi.org/10.1016/j.ecss.2019.03.023>
- 744 Ferronato, C., Falsone, G., Natale, M., Zannoni, D., Buscaroli, A., Vianello, G., Vittori Antisari, L., 2016. Chemical and pedological
745 features of subaqueous and hydromorphic soils along a hydrosequence within a coastal system (San Vitale Park, Northern Italy).
746 *Geoderma* 265, 141–151. <https://doi.org/10.1016/j.geoderma.2015.11.018>
- 747 Friedlingstein, P., Jones, M.W., O’Sullivan, M., Andrew, R.M., Hauck, J., Peters, G.P., Peters, W., Pongratz, J., Sitch, S., Le Quére,
748 C., Bakker, D.C.E., Canadell, J.G., Ciais, P., Jackson, R.B., Anthoni, P., Barbero, L., Bastos, A., Bastrikov, V., Becker, M., Bopp, L.,
749 Buitenhuis, E., Chandra, N., Chevallier, F., Chini, L.P., Currie, K.I., Feely, R.A., Gehlen, M., Gilfillan, D., Gkritzalis, T., Goll, D.S.,
750 Gruber, N., Gutekunst, S., Harris, I., Haverd, V., Houghton, R.A., Hurtt, G., Ilyina, T., Jain, A.K., Joetzjer, E., Kaplan, J.O., Kato, E.,
751 Goldewijk, K.K., Korsbakken, J.I., Landschützer, P., Lauvset, S.K., Lefèvre, N., Lenton, A., Lienert, S., Lombardozzi, D., Marland,
752 G., McGuire, P.C., Melton, J.R., Metzl, N., Munro, D.R., Nabel, J.E.M.S., Nakaoka, S.-I., Neill, C., Omar, A.M., Ono, T., Peregon,
753 A., Pierrot, D., Poulter, B., Rehder, G., Resplandy, L., Robertson, E., Rödenbeck, C., Séférian, R., Schwinger, J., Smith, N., Tans,
754 P.P., Tian, H., Tilbrook, B., Tubiello, F.N., R. van der Werf, G., Wiltshire, A.J., Zaehle, S., 2019. Global Carbon Project. (2019).
755 Supplemental data of Global Carbon Budget 2019 (Version 1.0) [Data set]. Global Carbon Project. <https://doi.org/10.18160/gcp-2019>
- 756 Gebrehiwet, T., Koretsky, C.M., Krishnamurthy, R. V., 2008. Influence of Spartina and Juncus on saltmarsh sediments. III. Organic
757 geochemistry. *Chem. Geol.* 255, 114–119. <https://doi.org/10.1016/j.chemgeo.2008.06.015>
- 758 Giordani, G., Viaroli, P., Swaney, D.P., Murray, C.N., Zaldívar, J.M., Marshall Crossland, J.I., 2005. Pialassa Baiona Lagoon,
759 Ravenna, Nutrient fluxes in transitional zones of the Italian coast. LOICZ Reports & Studies No. 28. LOICZ, Textel, the Netherlands.
- 760 Godin, P., Macdonald, R.W., Kuzyk, Z.Z.A., Goñi, M.A., Stern, G.A., 2017. Organic matter compositions of rivers draining into
761 Hudson Bay: Present-day trends and potential as recorders of future climate change. *J. Geophys. Res. Biogeosciences* 122, 1848–
762 1869. <https://doi.org/10.1002/2016JG003569>
- 763 Goñi, M.A., Ruttenberg, K.C., Eglinton, T.I., 1998. A reassessment of the sources and importance of land-derived organic matter in
764 surface sediments from the Gulf of Mexico. *Geochim. Cosmochim. Acta* 62, 3055–3075. [https://doi.org/10.1016/S0016-7037\(98\)00217-8](https://doi.org/10.1016/S0016-7037(98)00217-8)
- 765 Goñi, M.A., Teixeira, M.J., Perkeya, D.W., 2003. Sources and distribution of organic matter in a river-dominated estuary (Winyah
766 Bay, SC, USA). *Estuar. Coast. Shelf Sci.* 57, 1023–1048. [https://doi.org/10.1016/S0272-7714\(03\)00008-8](https://doi.org/10.1016/S0272-7714(03)00008-8)
- 767 Goñi, M.A., Thomas, K.A., 2000. Sources and transformations of organic matter in surface soils and sediments from a tidal estuary
768 (North Inlet, South Carolina, USA). *Estuaries* 23, 548–564. <https://doi.org/10.2307/1353145>
- 769 Guerra, R., Pasteris, A., Lee, S.-H., Park, N.-J., Ok, G., 2014. Spatial patterns of metals, PCDDs/Fs, PCBs, PBDEs and chemical
770 status of sediments from a coastal lagoon (Pialassa Baiona, NW Adriatic, Italy). *Mar. Pollut. Bull.* 89, 407–416.
771 <https://doi.org/10.1016/j.marpolbul.2014.10.024>
- 772 Guerra, R., Pasteris, A., Ponti, M., 2009. Impacts of maintenance channel dredging in a northern Adriatic coastal lagoon. I : Effects on
773 sediment properties , contamination and toxicity. *Estuar. Coast. Shelf Sci.* 85, 134–142. <https://doi.org/10.1016/j.ecss.2009.05.021>

- 776 Guerra, R., Pistocchi, R., Vanucci, S., 2013. Dynamics and sources of organic carbon in suspended particulate matter and sediments in
777 Pialassa Baiona lagoon (NW Adriatic Sea, Italy). *Estuar. Coast. Shelf Sci.* 135, 24–32. <https://doi.org/10.1016/j.ecss.2013.06.022>
- 778 Hama, T., Yanagi, K., Hama, J., 2004. Decrease in molecular weight of photosynthetic products of marine phytoplankton during early
779 diagenesis. *Limnol. Oceanogr.* 49, 471–481. <https://doi.org/10.4319/lo.2004.49.2.0471>
- 780 Hedges, J., Mann, D., 1979. The characterization of plant tissues by their lignin oxidation products. *Geochim. Cosmochim. Acta* 43,
781 1803–1807. [https://doi.org/https://doi.org/10.1016/0016-7037\(79\)90028-0](https://doi.org/https://doi.org/10.1016/0016-7037(79)90028-0)
- 782 Hedges, J.I., Clark, W.A., Quay, P.D., Richey, J.E., Devol, A.H., Santos, U.M., 1986. Composition and fluxes of particulate organic
783 material in the Amazon River. *Limnol. Oceanogr.* 31, 717–738.
- 784 Hensel, P.F., Day, J.W., Pont, D., 1999. Wetland vertical accretion and soil elevation change in the Rhone River Delta, France: The
785 importance of riverine flooding. *J. Coast. Res.* 15, 668–681.
- 786 Hill, T.D., Anisfeld, S.C., 2015. Coastal wetland response to sea level rise in Connecticut and New York. *Estuar. Coast. Shelf Sci.*
787 163, 185–193. <https://doi.org/10.1016/j.ecss.2015.06.004>
- 788 Huang, B., Thorne, P.W., Banzon, V.F., Boyer, T., Chepurin, G., Lawrimore, J.H., Menne, M.J., Smith, T.M., Vose, R.S., Zhang,
789 H.M., 2017. Extended reconstructed Sea surface temperature, Version 5 (ERSSTv5): Upgrades, validations, and intercomparisons. *J.*
790 *Clim.* 30, 8179–8205. <https://doi.org/10.1175/JCLI-D-16-0836.1>
- 791 Hughes, E.H., Sherr, E.B., 1983. Subtidal food webs in a georgia estuary: $\delta^{13}\text{C}$ analysis. *J. Exp. Mar. Bio. Ecol.* 67, 227–242.
792 [https://doi.org/10.1016/0022-0981\(83\)90041-2](https://doi.org/10.1016/0022-0981(83)90041-2)
- 793 INEMAR-ER, 2019. AGGIORNAMENTO DELL'INVENTARIO REGIONALE DELLE EMISSIONI IN ATMOSFERA
794 DELL'EMILIA-ROMAGNA RELATIVO ALL'ANNO 2015. Rapporto finale. [https://www.arpae.it/it/temi-
795 ambientali/aria/inventario-emissioni/inventario_emissioni_2015.pdf](https://www.arpae.it/it/temi-ambientali/aria/inventario-emissioni/inventario_emissioni_2015.pdf).
- 796 IPCC, 2019. IPCC, 2019: Summary for Policymakers, in: Pörtner, H.-O., Roberts, D.C., Masson-Delmotte, V., Zhai, P., Tignor, M.,
797 Poloczanska, E., Mintenbeck, K., Nicolai, M., Okem, A., Petzold, J., Rama, B., Weyer, N. (Eds.), IPCC Special Report on the Ocean
798 and Cryosphere in a Changing Climate.
- 799 Ishii, M., Shouji, A., Sugimoto, S., Matsumoto, T., 2005. Objective analyses of sea-surface temperature and marine meteorological
800 variables for the 20th century using ICOADS and the Kobe Collection. *Int. J. Climatol.* 25, 865–879. <https://doi.org/10.1002/joc.1169>
- 801 Jiménez-Arias, J.L., Morris, E., Rubio-de-Inglés, M.J., Peralta, G., García-Robledo, E., Corzo, A., Papaspyrou, S., 2020. Tidal
802 elevation is the key factor modulating burial rates and composition of organic matter in a coastal wetland with multiple habitats. *Sci.*
803 *Total Environ.* 724. <https://doi.org/10.1016/j.scitotenv.2020.138205>
- 804 Jones, M.L.M., Sowerby, A., Williams, D.L., Jones, R.E., 2008. Factors controlling soil development in sand dunes: Evidence from a
805 coastal dune soil chronosequence. *Plant Soil* 307, 219–234. <https://doi.org/10.1007/s11104-008-9601-9>
- 806 Kelleway, J.I., Saintilan, N., Macreadie, P.I., Baldock, J.A., Ralph, P.J., 2017. Sediment and carbon deposition vary among vegetation
807 assemblages in a coastal salt marsh. *Biogeosciences* 14, 3763–3779. <https://doi.org/10.5194/bg-14-3763-2017>
- 808 Kemp, A.C., Vane, C.H., Horton, B.P., Culver, S.J., 2010. Stable carbon isotopes as potential sea-level indicators in salt marshes,
809 North Carolina, USA. *Holocene* 20, 623–636. <https://doi.org/10.1177/0959683609354302>
- 810 Kemp, A.C., Vane, C.H., Horton, B.P., Engelhart, S.E., Nikitina, D., 2012. Application of stable carbon isotopes for reconstructing
811 salt-marsh floral zones and relative sea level, New Jersey, USA. *J. Quat. Sci.* 27, 404–414. <https://doi.org/10.1002/jqs.1561>
- 812 Khan, N.S., Vane, C.H., Horton, B.P., 2015a. Stable carbon isotope and C/N geochemistry of coastal wetland sediments as a sea-level
813 indicator. *Handb. Sea-Level Res.* 295–311. <https://doi.org/10.1002/9781118452547.ch20>
- 814 Khan, N.S., Vane, C.H., Horton, B.P., Hillier, C., Riding, J.B., Kendrick, C.P., 2015b. The application of $\delta^{13}\text{C}$, TOC and C/N
815 geochemistry to reconstruct Holocene relative sea levels and paleoenvironments in the Thames Estuary, UK. *J. Quat. Sci.* 30, 417–
816 433. <https://doi.org/10.1002/jqs.2784>
- 817 Kirwan, M.L., Megonigal, J.P., 2013. Tidal wetland stability in the face of human impacts and sea-level rise. *Nature* 504, 53–60.
818 <https://doi.org/10.1038/nature12856>
- 819 Kirwan, M.L., Mudd, S.M., 2012. Response of salt-marsh carbon accumulation to climate change. *Nature* 488, 550–553.
820 <https://doi.org/10.1038/nature11440>
- 821 Klap, V.A., Hemminga, M.A., Boon, J.J., 2000. Retention of lignin in seagrasses: Angiosperms that returned to the sea. *Mar. Ecol.*
822 *Prog. Ser.* 194, 1–11. <https://doi.org/10.3354/meps194001>
- 823 Kuzyk, Z.Z.A., Goñi, M.A., Stern, G.A., Macdonald, R.W., 2008. Sources, pathways and sinks of particulate organic matter in
824 Hudson Bay: Evidence from lignin distributions. *Mar. Chem.* 112, 215–229. <https://doi.org/10.1016/j.marchem.2008.08.001>
- 825 Lamb, A.L., Wilson, G.P., Leng, M.J., 2006. A review of coastal palaeoclimate and relative sea-level reconstructions using $\delta^{13}\text{C}$ and
826 C/N ratios in organic material. *Earth-Science Rev.* 75, 29–57. <https://doi.org/10.1016/j.earscirev.2005.10.003>
- 827 Legendre, P., Legendre, L., 2012. Numerical Ecology, 3rd editio. ed. Elsevier.
- 828 Li, Y., Von Storch, H., Wang, Q., Zhou, Q., Tang, S., 2019. Testing the validity of regional detail in global analyses of sea surface
829 temperature - The case of Chinese coastal waters. *Ocean Sci.* 15, 1455–1467. <https://doi.org/10.5194/os-15-1455-2019>
- 830 Lueker, T.J., Dickson, A.G., Keeling, C.D., 2000. Ocean pCO₂ calculated from dissolved inorganic carbon, alkalinity, and equations
831 for K₁ and K₂: Validation based on laboratory measurements of CO₂ in gas and seawater at equilibrium. *Mar. Chem.* 70, 105–119.
832 [https://doi.org/10.1016/S0304-4203\(00\)00022-0](https://doi.org/10.1016/S0304-4203(00)00022-0)
- 833 Macreadie, K.R.P.I., Saintilan, J.J.K.N., 2019. Blue carbon in coastal landscapes : a spatial framework for assessment of stocks and
834 additionality. *Sustain. Sci.* 14, 453–467. <https://doi.org/10.1007/s11625-018-0575-0>
- 835 Macreadie, P.I., Hughes, A.R., Kimbro, D.L., 2013. Loss of 'Blue Carbon' from Coastal Salt Marshes Following Habitat Disturbance.
836 *PLoS One* 8, 1–8. <https://doi.org/10.1371/journal.pone.0069244>

- 837 Mariano, C., Marino, M., Pisacane, G., Sannino, G., 2021. Sea Level Rise and Coastal Impacts: Innovation and Improvement of
838 the Local Urban Plan for a Climate-Proof Adaptation Strategy. *Sustainability* 13, 1565. <https://doi.org/10.3390/su13031565>
- 839 Mariotti, G., Carr, J., 2014. Dual role of salt marsh retreat: Long-term loss and short-term resilience. *Water Resour. Res.* 50, 2963–
840 2974. <https://doi.org/10.1002/2013WR014676>
- 841 Merloni, N., Piccoli, F., 1999. Carta della vegetazione - Parco regionale del Delta del Po - Stazione Pineta di San Vitale e Piassasse di
842 Ravenna (Digitale) - Edizione 1999.
- 843 Meyers, P.A., 1994. Preservation of elemental and isotopic source identification of sedimentary organic matter. *Chem. Geol.* 114,
844 289–302. [https://doi.org/10.1016/0009-2541\(94\)90059-0](https://doi.org/10.1016/0009-2541(94)90059-0)
- 845 Middelburg, J.J., Nieuwenhuize, J., Lubberts, R.K., Plassche, O. Van De, 1997. Organic Carbon Isotope Systematics of Coastal
846 Marshes. *Estuar. Coast. Shelf Sci.* 45, 681–687.
- 847 Mollema, P., Antonellini, M., 2012. Climate and water budget change of a Mediterranean coastal. *Env. Earth Sci* 65, 257–276.
848 <https://doi.org/10.1007/s12665-011-1088-7>
- 849 Mueller, P., Ladiges, N., Jack, A., Schmiedl, G., Kutzbach, L., Jensen, K., Nolte, S., 2019. Assessing the long-term carbon-
850 sequestration potential of the semi-natural salt marshes in the European Wadden Sea. *Ecosphere* 10. <https://doi.org/10.1002/ecs2.2556>
- 851 Negandhi, K., Edwards, G., Kelleway, J.J., Howard, D., Safari, D., Saintilan, N., 2019. Blue carbon potential of coastal wetland
852 restoration varies with inundation and rainfall. *Sci. Rep.* 1–9. <https://doi.org/10.1038/s41598-019-40763-8>
- 853 Oreska, M.P.J., Wilkinson, G.M., McGlathery, K.J., Bost, M., McKee, B.A., 2018. Non-seagrass carbon contributions to seagrass
854 sediment blue carbon. *Limnol. Oceanogr.* 63, S3–S18. <https://doi.org/10.1002/lno.10718>
- 855 Ouyang, X., Lee, S.Y., 2014. Updated estimates of carbon accumulation rates in coastal marsh sediments. *Biogeosciences* 11, 5057–
856 5071. <https://doi.org/10.5194/bg-11-5057-2014>
- 857 Palomo, L., Niell, F.X., 2009. Primary production and nutrient budgets of *Sarcocornia perennis* ssp. *alpini* (Lag.) Castroviejo in the
858 salt marsh of the Palmones River estuary (Southern Spain). *Aquat. Bot.* 91, 130–136. <https://doi.org/10.1016/j.aquabot.2009.04.002>
- 859 Pendleton, L., Donato, D.C., Murray, B.C., Crooks, S., Jenkins, W.A., Megonigal, P., Pidgeon, E., Herr, D., Gordon, D., Baldera, A.,
860 2012. Estimating Global “Blue Carbon” Emissions from Conversion and Degradation of Vegetated Coastal Ecosystems. *PLoS One*
861 7, 1–7. <https://doi.org/10.1371/journal.pone.0043542>
- 862 Pisano, A., Buongiorno Nardelli, B., Tronconi, C., Santoleri, R., 2016. The new Mediterranean optimally interpolated pathfinder
863 AVHRR SST Dataset (1982–2012). *Remote Sens. Environ.* 176, 107–116. <https://doi.org/10.1016/j.rse.2016.01.019>
- 864 Pisano, A., Marullo, S., Artale, V., Falcini, F., Yang, C., Leonelli, F.E., Santoleri, R., Nardelli, B.B., 2020. New evidence of
865 Mediterranean climate change and variability from Sea Surface Temperature observations. *Remote Sens.* 12, 1–18.
866 <https://doi.org/10.3390/RS12010132>
- 867 Ponti, M., Casselli, C., Abbiati, M., 2011. Anthropogenic disturbance and spatial heterogeneity of macrobenthic invertebrate
868 assemblages in coastal lagoons: The study case of Piasassa Baiona (northern Adriatic Sea). *Helgol. Mar. Res.* 65, 25–42.
869 <https://doi.org/10.1007/s10152-010-0197-0>
- 870 Preston, C.D., Pearman, A.D., Dines, D.T., 2002. *New Atlas of the British and Irish Flora*. Oxford University Press, Oxford.
- 871 Rayner, N.A., Parker, D.E., Horton, E.B., Folland, C.K., Alexander, L. V., Rowell, D.P., Kent, E.C., Kaplan, A., 2003. Global
872 analyses of sea surface temperature, sea ice, and night marine air temperature since the late nineteenth century. *J. Geophys. Res. D*
873 *Atmos.* 108, 1–22. <https://doi.org/10.1029/2002jd002670>
- 874 Rogers, K., Kelleway, J.J., Saintilan, N., Megonigal, J.P., Adams, J.B., Holmquist, J.R., Lu, M., Schile-beers, L., Zawadzki, A.,
875 Mazumder, D., Woodroffe, C.D., 2019. Wetland carbon storage controlled by millennial-scale variation in relative sea-level rise.
876 *Nature* 567, 91–96.
- 877 Roner, M., D’Alpaos, A., Ghinassi, M., Marani, M., Silvestri, S., Franceschinis, E., Realdon, N., 2016. Spatial variation of salt-marsh
878 organic and inorganic deposition and organic carbon accumulation: Inferences from the Venice lagoon, Italy. *Adv. Water Resour.* 93,
879 276–287. <https://doi.org/10.1016/j.advwatres.2015.11.011>
- 880 Ruiz-fernández, A.C., Carnero-bravo, V., Sanchez-cabeza, J.A., Pérez-bernal, L.H., Amaya-monterrosa, O.A., 2018. Carbon burial
881 and storage in tropical salt marshes under the influence of sea level rise. *Sci. Total Environ.* 630, 1628–1640.
882 <https://doi.org/10.1016/j.scitotenv.2018.02.246>
- 883 Saintilan, N., Rogers, K., Mazumder, D., Woodroffe, C., 2013. Allochthonous and autochthonous contributions to carbon
884 accumulation and carbon store in southeastern Australian coastal wetlands. *Estuar. Coast. Shelf Sci.* 128, 84–92.
885 <https://doi.org/10.1016/j.ecss.2013.05.010>
- 886 Sanchez-Cabeza, J.A., Ruiz-Fernandez, A.C., 2012. Pb sediment radiochronology : An integrated formulation and classification of
887 dating models. *Geochim. Cosmochim. Acta* 82, 183–200. <https://doi.org/10.1016/j.gca.2010.12.024>
- 888 Simpson, L.T., Osborne, T.Z., Duckett, L.J., Feller, I.C., 2017. Carbon Storages along a Climate Induced Coastal Wetland Gradient.
889 *Wetlands* 37, 1023–1035. <https://doi.org/10.1007/s13157-017-0937-x>
- 890 Sousa, A.I., Lillebø, A.I., Pardal, M.A., Caçador, I., 2010. The influence of *Spartina maritima* on carbon retention capacity in salt
891 marshes from warm-temperate estuaries. *Mar. Pollut. Bull.* 61, 215–223. <https://doi.org/10.1016/j.marpolbul.2010.02.018>
- 892 Sousa, A.I., Santos, D.B., Silva, E.F. Da, Sousa, L.P., Cleary, D.F.R., Soares, A.M.V.M., Lillebø, A.I., 2017. ‘Blue Carbon’ and
893 Nutrient Stocks of Salt Marshes at a Temperate Coastal Lagoon (Ria de Aveiro, Portugal). *Sci. Rep.* 7, 1–11.
894 <https://doi.org/10.1038/srep41225>
- 895 Spivak, A.C., Sanderman, J., Bowen, J.L., Canuel, E.A., Hopkinson, C.S., 2019. Global-change controls on soil-carbon accumulation
896 and loss in coastal vegetated ecosystems. *Nat. Geosci.* 12, 685–692. <https://doi.org/10.1038/s41561-019-0435-2>
- 897 Storto, A., Bonaduce, A., Feng, X., Yang, C., 2019. Steric Sea Level Changes from Ocean Reanalyses at Global and Regional Scales.

- 898 Water, 11(10), 1987. <https://doi.org/10.3390/w11101987>.
- 899 Tan, L., Ge, Z., Tang, J., Zhou, X., Li, S., Li, X., 2020. Conversion of coastal wetlands , riparian wetlands , and peatlands increases
900 greenhouse gas emissions : A global 1638–1653. <https://doi.org/10.1111/gcb.14933>
- 901 Tanner, B.R., Uhle, M.E., Kelley, J.T., Mora, C.I., 2007. C3/C4 variations in salt-marsh sediments: An application of compound
902 specific isotopic analysis of lipid biomarkers to late Holocene paleoenvironmental research. *Org. Geochem.* 38, 474–484.
903 <https://doi.org/10.1016/j.orggeochem.2006.06.009>
- 904 Tanner, B.R., Uhle, M.E., Mora, C.I., Kelley, J.T., Schuneman, P.J., Lane, C.S., Allen, E.S., 2010. Comparison of bulk and
905 compound-specific $\delta^{13}\text{C}$ analyses and determination of carbon sources to salt marsh sediments using n-alkane distributions (Maine,
906 USA). *Estuar. Coast. Shelf Sci.* 86, 283–291. <https://doi.org/10.1016/j.ecss.2009.11.023>
- 907 Tsimplis, M.N., Raicich, F., Fenoglio-marc, L., Shaw, A.G.P., Marcos, M., Somot, S., Bergamasco, A., 2012. Recent developments in
908 understanding sea level rise at the Adriatic coasts. *Phys. Chem. Earth* 40–41, 59–71. <https://doi.org/10.1016/j.pce.2009.11.007>
- 909 USEPA, 2000. METHOD 6010C. INDUCTIVELY COUPLED PLASMA-ATOMIC EMISSION SPECTROMETRY. p. 30.
- 910 Van de Broek, M., Baert, L., Temmerman, S., Govers, G., 2019. Soil organic carbon stocks in a tidal marsh landscape are dominated
911 by human marsh embankment and subsequent marsh progradation. *Eur. J. Soil Sci.* 70, 338–349. <https://doi.org/10.1111/ejss.12739>
- 912 Van De Broek, M., Temmerman, S., Merckx, R., Govers, G., 2016. Controls on soil organic carbon stocks in tidal marshes along an
913 estuarine salinity gradient. *Biogeosciences* 13, 6611–6624. <https://doi.org/10.5194/bg-13-6611-2016>
- 914 Wakeham, S.G., Lee, C., Hedges, J.I., Hernes, P.J., Peterson, M.L., 1997. Molecular indicators of diagenetic status in marine organic
915 matter. *Geochim. Cosmochim. Acta* 61, 5363–5369. [https://doi.org/10.1016/S0016-7037\(97\)00312-8](https://doi.org/10.1016/S0016-7037(97)00312-8)
- 916 Wang, F., Lu, X., Sanders, C.J., Tang, J., 2019. Tidal wetland resilience to sea level rise increases their carbon sequestration capacity
917 in United States. *Nat. Commun.* 10, 1–11. <https://doi.org/10.1038/s41467-019-13294-z>
- 918 Ward, R.D., 2020. Carbon sequestration and storage in Norwegian Arctic coastal wetlands: Impacts of climate change. *Sci. Total*
919 *Environ.* 748, 141343. <https://doi.org/10.1016/j.scitotenv.2020.141343>
- 920 Wilkinson, G.M., Besterman, A., Buelo, C., Gephart, J., Pace, M.L., 2018. A synthesis of modern organic carbon accumulation rates
921 in coastal and aquatic inland ecosystems. *Sci. Rep.* 8, 1–9. <https://doi.org/10.1038/s41598-018-34126-y>
- 922 Wilson, G.P., 2017. On the application of contemporary bulk sediment organic carbon isotope and geochemical datasets for Holocene
923 sea-level reconstruction in NW Europe. *Geochim. Cosmochim. Acta* 214, 191–208. <https://doi.org/10.1016/j.gca.2017.07.038>
- 924 Winogradow, A., Pempkowiak, J., 2014. Organic carbon burial rates in the Baltic Sea sediments. *Estuar. , Coast. Shelf Sci.* 138, 27–
925 36.
- 926 World Bank, 2019. ‘CO2 Emissions (Metric Tons Per Capita).’ *World Development Indicators*.
- 927 Zerbini, S., Raicich, F., Maria, C., Bruni, S., Del, S., Errico, M., 2017. Earth-Science Reviews Sea-level change in the Northern
928 Mediterranean Sea from long-period tide gauge time series 167, 72–87. <https://doi.org/10.1016/j.earscirev.2017.02.009>
- 929
930
931
932

933 Table 2. Carbon accumulation rates ($\text{g OC m}^{-2} \text{yr}^{-1}$) in coastal wetlands in European Seas and worldwide averages.
 934

Area	type	time span	OC accumulation rate ($\text{g m}^{-2} \text{yr}^{-1}$)	Dominant halophyte species/genera	Reference
Global (coastal and inland ecosystems)	sediment	<200 yr	15.6 - 73.2	<i>various</i>	(Wilkinson et al., 2018)
NW Atlantic	tidal wetlands soil	ca 100-150 yrs	172.2±18.1	<i>various</i>	(Ouyang and Lee, 2014)
US tidal wetlands	salt marsh sediments	nr ^a	154.3±8	<i>various</i>	(Wang et al., 2019)
<i>NE Atlantic</i>					
Norwegian Arctic coastal wetlands	low marsh	ca 100 yrs	19-390	<i>Juncus gerardii</i>	(Ward, 2020)
North Sea and Skagerrak Sea	continental shelf	ca 100 yrs	0.02-66.18	nr	(Diesing et al., 2021)
Baltic Sea	continental shelf, estuaries, fjords	nr	13–54	nr	(Winogradow and Pempkowiak, 2014)
Wadden Sea, Germany	semi-natural salt marsh	ca 50 yrs	112-149	<i>Spartina anglica, Salicornia europaea, Puccinellia maritima</i>	(Mueller et al., 2019)
Coastal margin habitats, UK	dry dune habitat	140 yrs	58±26	<i>Carex arenaria, Hypochaeris radicata, Ammophila arenaria</i>	(Jones et al., 2008)
	wet dune habitat	140 yrs	73.0±22	<i>Carex arenaria, Hypochaeris radicata, Ammophila arenaria</i>	(Jones et al., 2008)
	salt marsh	60 yrs	64-219	nr	(Beaumont et al., 2014)
	machair	60 yrs	34.9±15.7	nr	(Beaumont et al., 2014)
Blackwater Estuary, England	salt marsh	ca 10 yrs	6.1-66	<i>Salicornia</i> spp., <i>Spartina</i> spp., <i>Aster tripolium</i> , <i>Puccinellia maritima</i>	(Adams et al., 2012)
Scheldt estuary, Netherlands	salt marsh	<60 yrs	88-151	<i>E. athericus</i>	(Van De Broek et al., 2016)

	salt marsh	<60 yrs	2177 ± 503	<i>Spartina anglica</i>	(Van De Broek et al., 2016)
	salt marsh	<60 yrs	22 ± 10	<i>Mixed vegetation</i>	(Van De Broek et al., 2016)
	embanked salt marsh	<64 yr	86.6± 7.5	nr	(Van de Broek et al., 2019)
	embanked brackish marsh	ca 100 yrs	111.3± 11.4	nr	(Van De (Van de Broek et al., 2019)
Guadiana Estuary, Portugal	salt marsh	13,000 - 6900 cal yrs BP	164-314	nr	(Boski et al., 2021)
Guadiana Estuary, Portugal	salt marsh	after 6900 cal yrs BP	46-52	nr	(Boski et al., 2021)
Mondego Estuary, Portugal	salt marsh	2 yrs	<100	<i>Scirpus maritimus</i>	(Couto et al., 2013)
	salt marsh	2 yrs	100-200	<i>Spartina maritima</i>	(Couto et al., 2013)
	salt marsh	2 yrs	300-400	<i>Zoostera nolti, Spartina maritima</i>	(Couto et al., 2013)
	salt marsh	2 yrs	213-218	<i>Spartina maritima</i>	(Sousa et al., 2010)
Tagus Estuary, North East Atlantic	salt marsh	<100 yrs	150-340	<i>Spartina maritima, Halimione portulacoides</i>	(Caçador et al., 2004)
Ria de Aveiro, Portugal	low marsh	nr	119.5 ± 5.3	<i>Spartina maritima</i>	(Sousa et al., 2017)
Ria de Aveiro, Portugal	mid & high marsh	nr	132.7 ± 5.8	<i>Juncus maritimus</i>	(Sousa et al., 2017)
Ria de Aveiro, Portugal	mid & high marsh	nr	157.3	<i>Halimione portulacoides</i>	(Sousa et al., 2017)
Ria de Aveiro, Portugal	mid & high marsh	nr	152	<i>Sarcoconia perennis</i>	(Sousa et al., 2017)

Odiel marshes	salt marsh	2-3 yrs	104	<i>Spartina maritima</i>	(Curado et al., 2013)
Bay of Cadiz, Spain	tidal coastal wetland	ca 100 yrs	40-107	<i>Spartina maritima</i> , <i>Zoostera nolstei</i>	(Jiménez-Arias et al., 2020)
Palomones Estuary	salt marsh	nr	560	<i>Sarcoconia perennis</i>	(Palomo and Niell, 2009)
<i>Mediterranean Sea</i>					
Venice lagoon, North Adriatic, Italy	salt marsh	nr	132	<i>Salicornia veneta</i> , <i>Spartina maritima</i> , <i>Limonium narbonense</i> , <i>Sarcocornia fruticosa</i> , <i>Juncus maritimus</i>	(Roner et al., 2016)
Rhône River Delta, France	riverine sites	3 yrs	357	<i>Juncus maritimus</i> , <i>Phragmites australis</i> , <i>Scirpus lacustris</i> , <i>Scirpus litoralis</i>	(Hensel et al., 1999)
	marine sites	3 yrs	87.9	<i>Arthrocnemum fruticosum</i> , <i>Halmione portulacoides</i> , <i>Suaeda fruticosa</i> , <i>Limonium vulgare</i>	(Hensel et al., 1999)
	impounded sites	3 yrs	72.1	<i>Juncus maritimus</i> , <i>Arthrocnemum fruticosum</i>	(Hensel et al., 1999)
Ebro River Delta, Spain	tidal marsh	ca 3 yrs	94-126	<i>Phragmites australis</i> , <i>Tipha</i> spp.	(Calvo-Cubero et al., 2014)
	salt marsh	<100 yr	39-293	<i>Sarcoconia fruticosa</i>	(Fennessy et al., 2019)
	brackish marsh	<100 yr	32-495	<i>Phragmites australis</i> , <i>Cladium mariscus</i> , <i>Juncus maritimus</i> , <i>Sarcocornia fruticosa</i> , <i>Scirpus maritimus</i> , <i>Spartina versicolor</i> , <i>Paspalum</i> spp.	(Fennessy et al., 2019)